DAHLGREN DIVISION
NAVAL SURFACE WARFARE CENTER
Dahlgren, Virginia 22448-5100

NSWCDD/TR-96/240

AN IMPROVED METHOD FOR PREDICTING AXIAL FORCE AT HIGH ANGLE OF ATTACK

BY FRANK G. MOORE TOM HYMER

WEAPONS SYSTEMS DEPARTMENT

FEBRUARY 1997

REPORT DOCUMENTATION PAGE

Form Approved
OMB No. 0704-0188

1. AGENCY USE ONLY (Leave blank)	2. REPORT DATE	3. REPORT TYPE AND DATES COVERED
	Feb. 97 ~~December 1996~~	Final

4. TITLE AND SUBTITLE

An Improved Method for Predicting Axial Force at High Angle of Attack

5. FUNDING NUMBERS

6. AUTHOR(s)

Frank G. Moore, Tom Hymer

7. PERFORMING ORGANIZATION NAME(S) AND ADDRESS(ES)

Commander
Naval Surface Warfare Center
Dahlgren Division (Code G04)
17320 Dahlgren Road
Dahlgren, VA 22448-5100

8. PERFORMING ORGANIZATION REPORT NUMBER

NSWCDD/TR-96/240

9. SPONSORING/MONITORING AGENCY NAME(S) AND ADDRESS(ES)

10. SPONSORING/MONITORING AGENCY REPORT NUMBER

11. SUPPLEMENTARY NOTES

12a. DISTRIBUTION/AVAILABILITY STATEMENT

Approved for public release; distribution is unlimited.

12b. DISTRIBUTION CODE

13. ABSTRACT (Maximum 200 words)

An improved semiempirical method for axial force calculation on missile configurations has been developed. The method uses the theoretical methods currently used in the Naval Surface Warfare Center Aeroprediction Code for zero angle-of-attack (AOA) axial force computations and several wind tunnel data bases to compute changes in axial force at AOA. The method is applicable to bodies alone, wing-body, and wing-body-tail configurations for both zero and non-zero control deflections. It has been developed to allow computation for AOA to 90 deg at any Mach number. However, it has been validated against data only to Mach number of 4.6 and AOA to 40 deg for all configurations. For body alone and wing-body cases, it has been validated to 90 deg AOA. Additional test data or Navier Stokes computations would allow refinement of the improved method.

The new method has been compared to several existing techniques. The method was found to be as good as or better than existing techniques, but more general than existing methods in terms of configurations and Mach numbers allowed for the method to be used.

14. SUBJECT TERMS

Aeroprediction Code, AP95, wing-body-tail configuration, body loading, linear load, non-linear load, normal force, wing-alone normal force, bending moment, wing deflection

15. NUMBER OF PAGES

63

16. PRICE CODE

17. SECURITY CLASSIFICATION OF REPORTS	18. SECURITY CLASSIFICATION OF THIS PAGE	19. SECURITY CLASSIFICATION OF ABSTRACT	20. LIMITATION OF ABSTRACT
UNCLASSIFIED	UNCLASSIFIED	UNCLASSIFIED	UL

FOREWORD

The 1995 version of the Aeroprediction Code (AP95) extended the code's angle-of-attack (AOA) capability to 90 deg through empirical additions to normal force of various missile components based on several large wind tunnel data bases. However, very little emphasis was placed on improving the axial force coefficient at high AOA. The justification for this was that normal force was by far the dominant term and axial force only a minor contributor to lift and drag. While this statement is still true, it is less true at subsonic speeds and therefore can result in appreciable errors in axial force and drag prediction at high AOA. As a result, new technology has been developed to remedy this problem. This new technology is discussed in this report.

The work described in this report was supported through the Office of Naval Research (Mr. Dave Siegel) by the following programs: the Air Launched Weapons Program managed at the Naval Air Warfare Center, China Lake, CA, by Mr. Tom Loftus and Dr. Craig Porter, and the Surface Weapons Systems Technology Program managed at the Naval Surface Warfare Center, Dahlgren Division (NSWCDD) by Mr. Robin Staton and Mr. Gil Graff. Also, some support was provided by the Marine Corps Weaponry Technology Program managed at NSWCDD by Mr. Bob Stiegler. The authors express appreciation for support received in this work.

Approved by:

DAVID S. MALYEVAC, Deputy Head
Weapons Systems Department

CONTENTS

ILLUSTRATIONS

ILLUSTRATIONS (Continued)

TABLES

1.0 INTRODUCTION

The latest version of the Aeroprediction Code (AP95)[1] available to the public places a lot of emphasis on zero lift drag or axial force coefficient at zero angle of attack (AOA) with only minor attention devoted to the change in C_A with AOA. One component of C_A, the base axial force coefficient change with AOA, is treated in a fairly comprehensive manner. The primary rationale for not devoting more effort to calculating the change in total axial force with AOA is the fact that for most conditions, normal force is the dominant term in lift, drag, and lift/drag ratio at high AOA, and C_A plays a secondary role. However at subsonic Mach numbers, C_A can actually go negative at high AOA, causing more error in C_L, C_D, and L/D than desired. Also, at very high Mach numbers ($M > 3.0$), C_A tends to increase with AOA much more than the current AP95 predicts. Finally, the change in C_A with control deflection, while predicted reasonably well by the AP95, could possibly be improved somewhat, also at subsonic and high supersonic conditions. It is therefore the intent of this report to discuss the physics of the changes in axial force with AOA, develop a semiempirical mathematical model to account for the physics, and compare the improved axial force model at AOA with the AP95 and experimental data.

In researching the literature for methods to account for axial force changes with AOA, three were found. The first of these was by Jorgensen[2] where he approximated C_A by:

$$C_A \simeq C_{A_0} \cos^2\alpha \; ; \; 0 \leq \alpha \leq 90^\circ \tag{1}$$

This method worked reasonably well for subsonic Mach numbers and AOAs less than about 30 deg. References 3 and 4 improved upon the Jorgensen method by assuming

$$C_A = C_{A_0} + f(M,\alpha) \tag{2}$$

$f(M,\alpha)$[3] was approximated by a fourth order polynomial in AOA for subsonic and transonic Mach numbers and was assumed to be zero[4] for supersonic Mach numbers. This was an improvement on the Jorgensen methodology at all Mach numbers and particularly for AOAs greater than about 30 deg. However, since $f(M,\alpha) = 0$ at $M \geq 1.5$, the method did not pick up the increase in C_A due to compressibility effects at higher M. Reference 5 then improved upon Reference 4 by assuming $f(M,\alpha)$ was second order in AOA at supersonic Mach numbers for bodies alone and third order for wing-bodies. Unlike Reference 1, which gives consistently accurate results for C_{A_0}, using second order methods, References 2 through 5 all use basically empirical methods for computing C_{A_0}. This means the empirical methods are limited to the data bases upon which they are based, not only at high AOA,

but low AOA as well. Furthermore, neither References 4 or 5 treated wing-body-tail configurations separately from wing-body cases.

While References 4 and 5 give acceptable accuracy for f(M,α) at AOAs to 90 deg for body alone and body-tail cases, they use different prediction methods in various Mach number regions. It is the goal of the present work to derive a single new function, f(M,α), that is as accurate or more accurate than either the Reference 4 or 5 methods, yet is applicable over the entire Mach number and AOA range of interest and is applicable to body alone, wing-body, or wing-body-tail cases. In addition, neither Reference 2, 4, or 5 treated empirical corrections to axial force on missile configurations with combined AOA and control deflection. This area will also be investigated for possible improvement.

2.0 ANALYSIS

2.1 REVIEW OF C_{A_0} METHODOLOGY IN THE AP95

Equation (2) will be assumed to apply for both body alone, and configurations with lifting surfaces as well. The AP95 methodology for C_{A_0} of Equation (2) is based on computing independently the wave or pressure axial force, skin-friction and base term.[1] The wave drag term is computed at low supersonic Mach numbers by combining modified Newtonian theory (MNT) with Second-Order Van Dykes hybrid theory,[6] at moderate supersonic Mach numbers by improvements to second-order, shock expansion theory combined with MNT,[7] and at Hypersonic Mach numbers by further refinements in shock expansion theory and MNT extended to real gases.[8] The combination of the above new methods developed during the course of the AP95 development has allowed zero lift drag to be computed with average accuracies generally of ±10 percent for a broad range of configurations and for Mach numbers ≥1.2. Configurations can have truncated, spherically blunt or sharp noses with boattails or flares. Additionally, up to two discontinuities in surface slope are allowed along the nose of the body.

At subsonic Mach numbers, the pressure component of axial force is assumed to be zero except in cases where a large cone half angle exists on the nose, creating a separation bubble in the vicinity of the nose or on truncated noses. The viscous separation term is estimated empirically.[6] At transonic Mach numbers, the wave drag is estimated analytically by either the method of Wu and Aoyoma[9] or using an unsteady solution of the Euler equations.[10] These estimates of wave drag were then included in table lookup form into the AP95[6,11] as functions of nose length, bluntness and Mach number. Boattail effects were computed by the Reference 9 methodology.

The skin-friction drag was computed by the Van Driest II method[12] for the turbulent portion of the boundary layer. The laminar portion is based on the incompressible flow over a flat plate and modified for compressibility in Reference 1. The AP95 allows various options for surface conditions including typical flight, wind tunnel model with and without a boundary layer trip, and all laminar flow. These options affect the transition Reynolds number where the flow becomes turbulent.

The base drag is computed empirically as a function of AOA, Mach number, fin location, fin thickness effects, fin control deflection, and boattail and for both power on or off conditions. The methodology is given in Reference 13 and was upgraded from the original AP72[6] by new wind tunnel data described in Reference 13.

Fin effects on C_{A_0} are computed in a similar way to the body alone. There are a couple of differences however. For blunt leading edge wings, the MNT is combined with first order versus second order perturbation theory. This can be done for two reasons. First, the wing drag is generally much smaller than the body drag. Secondly, the wings generally are thin, thus having frontal areas with smaller slopes than the body. This allows first order perturbation theory to yield acceptable wave drag on wings. The second difference between the C_{A_0} of wings and bodies is the wing trailing edge drag versus body base drag. The body base drag uses a three-dimensional base pressure coefficient whereas a two-dimensional base pressure coefficient is used for a blunt wing trailing edge.

As is apparent from the discussion on C_{A_0}, the AP95 has placed a major emphasis on accurate values of C_{A_0} from its inception in 1972. The reason for this goes back to the fact that in 1972, there was no accurate way to calculate drag of spin-stabilized projectiles for range estimation. To put the level of emphasis on C_{A_0} in context of the overall AP95, consider the following. The AP95 contains 135 primary subroutines consisting of over 16000 lines of code. It is estimated that about half the code is for computing accurate values of C_{A_0}. One simply cannot get accurate values of C_{A_0} for a broad class of body shapes by empirical or first order perturbation methods. Second-order perturbation methods, in combination with modified Newtonian theory, and judicious selection of a match point between Newtonian and the second-order method is the lowest order analytical method acceptable for projectile and missile range estimation in general.

2.2 C_A PHYSICAL PHENOMENA AT AOA

Before developing a mathematical model to address changes in axial force coefficient as a function of AOA, it is appropriate to discuss the physics of the flow that causes these changes. To visualize the changes, the axial force will be once again broken down into its components due to pressure, skin-friction and base drag.

For subsonic Mach numbers and spherically blunt or ogive shaped bodies, the pressure drag at low to moderate AOA is zero. However, as AOA is increased or for bodies with truncated noses or large cone half angles, the flow forms a separation bubble in the vicinity of the nose region. This separation bubble has a negative pressure coefficient, which means the axial force decreases with AOA. On the other hand, at high Mach number, the pressure coefficient on the windward side of the body is a function of the sine squared of the angle between a tangent to the body surface and the velocity vector. This means the increase in axial force at high Mach number with AOA is positive due to compressibility effects of the air. On the leeward surface of the body, the pressure coefficient approaches zero at high Mach number so it has little effect on the axial force coefficient. None of the theoretical methods being used for computing the pressure component of the axial force coefficient accurately account for these changes above AOA of about 10 deg.

The base axial force changes with AOA are positive at all Mach numbers[13] but are the largest at transonic Mach numbers. At very high Mach numbers where the base term approaches zero, the change with AOA is also zero. At moderate AOA, the increase in base axial force reaches a maximum and then begins decreasing with additional increases in AOA. When fins are placed on the body in the vicinity of the base, the increase in base axial force with AOA is mitigated substantially. It is not clear the phenomena that cause these effects with AOA. It is suspected that for the body alone, the initial AOA increases cause a stronger separation at the shoulder due to a larger turn angle at the base. However, when fins are placed in the vicinity of the base, it is suspected that some of the high dynamic pressure fluid is channeled into the base region, thus mitigating the negative base pressure coefficient somewhat.

The skin-friction coefficient axial force change with AOA is even harder to estimate or to explain, due to the lack of CFD or wind tunnel data which attempt to measure this quantity at moderate to high AOA. At lower Mach number where strong separation exists in the leeward plane area along with a fairly large reverse flow region, it is suspected that the skin friction decreases with AOA. As Mach number increases, the reverse flow region decreases and the change in skin friction axial force with AOA is probably nearly constant or maybe slightly positive for low to moderate AOAs.

Another physical phenomena which causes changes in C_A (at moderate and higher supersonic Mach numbers) with AOA is internal shock interactions. These phenomena are primarily associated with bodies with lifting surfaces and particularly those with more than one set. The body alone generally will have only a bow shock and internal expansion waves unless there is a surface discontinuity present. A body-tail configuration will have shocks coming off the tail surfaces which interact with the bow shock. At Mach numbers and AOAs high enough, these interactions can have an impact on the axial force. Finally, if two or more sets of lifting surfaces are present, even stronger shock interactions occur between not only the bow and wing shock but wing to tail shocks as well. The situation is further complicated if a control surface is deflected. The internal shock interaction effects can affect the other static aerodynamics as well as axial force when this is the case.

2.3 IMPROVED SEMIEMPIRICAL AOA THEORETICAL MODEL

As stated in the Introduction section of the report, the goal is to develop a single method to predict $f(M,\alpha)$ of Equation (2) as accurate as either of the methods in References 4 and 5, but which applies for all Mach numbers for bodies with and without lifting surfaces, and for AOA to 90 deg. To this end, we assume

$$f(M,\alpha) = A\alpha + B\alpha^2 + C\alpha^3 + D\alpha^4 \qquad (3)$$

To evaluate the coefficients A, B, C, and D require four independent conditions. These conditions are:

i) $\left.\frac{\partial f}{\partial \alpha}\right|_{\alpha=0} = f'(M,0)$

ii)-iv) The value of f(M,α) at α = 30 deg, 60 deg and 90 deg respectively.

Using these four conditions, and putting α in radians versus degrees, four equations are arrived at to solve simultaneously. These equations are:

$$\begin{aligned} A &= f'(M,0) \\ .524A + .274B + .144C + .076D &= f(M,30) \\ 1.047A + 1.096B + 1.148C + 1.202D &= f(M,60) \\ 1.571A + 2.467B + 3.875C + 6.059D &= f(M,90) \end{aligned} \tag{4}$$

Simultaneous solution of the variables A, B, C, and D from Equation (4) gives

$$\begin{aligned} A= &\quad f'(M,0) \\ B= &-3.509\ f'(M,0) + 11.005\ f(M,30) - 2.757\ f(M,60) + 0.41\ f(M,90) \\ C= &\quad 3.675\ f'(M,0) - 17.591\ f(M,30) + 7.041\ f(M,60) - 1.179\ f(M,90) \\ D= &-1.181\ f'(M,0) + 6.771\ f(M,30) - 3.381\ f(M,60) + .752\ f(M,90) \end{aligned} \tag{5}$$

Knowing f'(M,0), f(M,30), f(M,60) and f(M,90) in conjunction with Equations (5), (3) and (2), improved estimates of C_A at AOAs up to 90 deg should be obtained. In reality, if the body is symmetric, then this AOA should be ±90 so long as Equation (3) is viewed in terms of absolute values for AOA.

The question that must be addressed is how to determine values of the parameters f'(M,0), f(M,30), f(M,60) and f(M,90). To do this, two large wind tunnel data bases were utilized. These were the NASA Tri-Service Data Base,[14] which contains detailed missile component data to AOA 45 deg, and the Baker[15] high AOA data base, which includes missile component data to 180 deg AOA. Reference 14 was used primarily for the lower AOA information, f'(M,0) and f(M,30), and Reference 15 was used for the higher AOA variables, f(M,60) and f(M,90). The reason for this was that Reference 14 data were available in tabular form making the estimates of the parameters more accurate than from the Reference 15 information, which was available only in graphs. For some data points in the transonic flow region, the parameter f(M,30) was obtained by averaging the data from both References 14 and 15.

Figure 1 gives the values of the parameters f'(M,0), f(M,30), f(M,60) and f(M,90) for the body alone. Reference 5 indicated analysis showed the first parameter (f'(M,0)) was independent of nose length, nose shape, and total body length and dependent only on Mach number. This assumption will also be made for the other three parameters as well. Comparison of the new method on configurations different from those within the data base will determine the validity of this assumption. Table 1 gives the values of the body alone parameters of Figure 1.

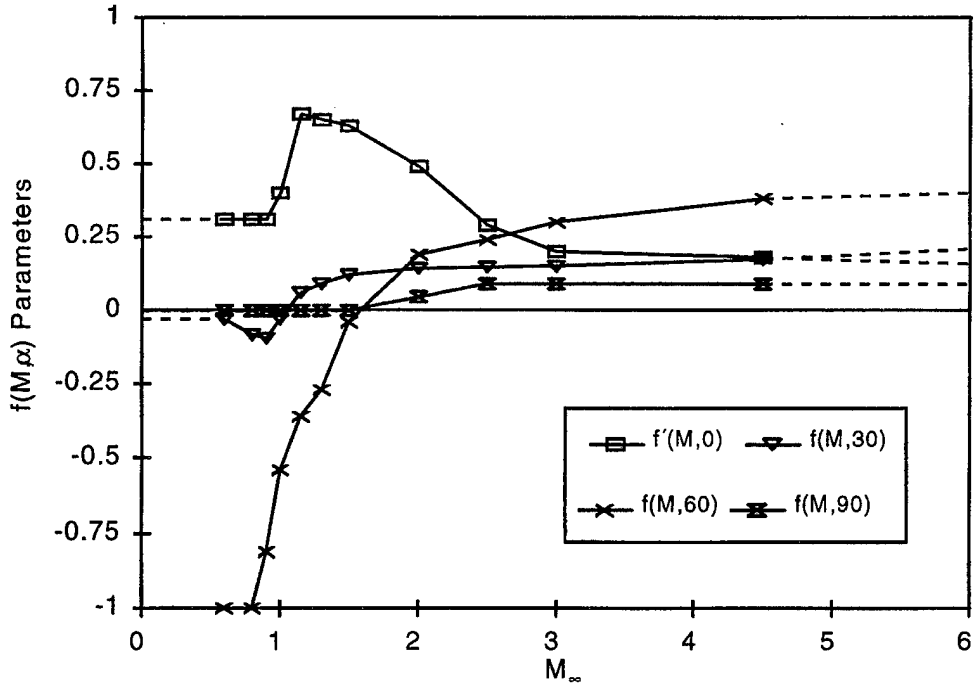

FIGURE 1. AXIAL FORCE AOA VARIATION PARAMETERS FOR BODY ALONE

TABLE 1. VALUES OF THE AXIAL FORCE AOA PARAMETERS FOR A BODY ALONE CONFIGURATION

M	f'(M,0)/rad	f(M,30)	f(M,60)	f(M,90)
0	0.31	-0.030	-1.00	0
0.6	0.31	-0.030	-1.00	0
0.8	0.31	-0.083	-1.00	0
0.9	0.31	-0.095	-0.81	0
1.0	0.40	-0.030	-0.54	0
1.15	0.67	0.060	-0.36	0
1.3	0.65	0.090	-0.27	0
1.5	0.63	0.120	-0.04	0
2.0	0.49	0.142	0.19	0.045
2.5	0.29	0.147	0.24	0.090
3.0	0.20	0.150	0.30	0.090
4.5	0.18	0.173	0.38	0.090
≥6.0	0.16	0.210	0.40	0.090

Figure 2 and Table 2 give the values of the same parameters for a configuration with one set of lifting surfaces. These parameters were derived for mostly body-tail configurations. In comparing values of the parameters in Figure 2 with those of Figure 1, it is seen that similar values exist for each parameter but they are slightly different. The Reference 4 method shows no difference between configurations that are bodies alone versus those with lifting surfaces, and Reference 5 shows a difference only as AOA approaches 90 deg. Thus the present method will also give slightly different results for body alone and wing-body or body-tail missile configurations than those of References 4 and 5 due to differences in the values of the parameters used in defining the nonlinearity with AOA. This is in addition to differences arising from the use of a single equation for all cases in the present approach versus three different equations used in References 4 and 5.

Unfortunately, neither of the data bases given in References 14 or 15 tested configurations with two sets of lifting surfaces. While the coefficients defined by Figure 2 and Table 2 could be used as an approximation for configurations with two sets of lifting surfaces, it will be attempted to improve upon these, at least for the lower AOAs where other data are available. To this end, References 17 through 20 were utilized. References 17 and 18 were very helpful in defining f'(M,0) and f(M,30) for Mach numbers 0.8 to 4.6. Above 4.6, values of these parameters were extrapolated as was done in Tables 1 and 2 as well. References 19 and 20 were utilized for low Mach number values of f'(M,0), f(M,30) and f(M,60). f(M,60) for high Mach numbers could be extrapolated reasonably well based on the Reference 18 data in conjunction with Figure 2. The f(M,90) data are simply a best guess based on f(M,60) values for wing-body-tail cases and f(M,60) and f(M,90) values of Table 2.

Values of the four parameters of Equation (5) are given in Figure 3 and Table 3 for configurations having two sets of lifting surfaces. In comparing Figures 2 and 3, it is seen there are some similarities but also some differences. At low Mach numbers, trends of all four parameters are similar, which means that Table 2 could be used successfully for configurations with more than one set of lifting surfaces and still get reasonably accurate estimates of axial force change with AOA. This is in fact what References 4 and 5 both do. However, as Mach number increases, values of the parameters f'(M,0) and f(M,30) tend to be higher for two sets of lifting surfaces compared to one. That is, C_A increases faster and reaches a higher peak value with AOA for a wing-body-tail case than for a wing-body or body-tail case.

The last physical phenomena to be modeled is the change in axial force coefficient with control deflection as AOA increases. The AP95 defines the axial force term due to control deflection as

$$C_{A_{\delta_W}} = C_{N_{W(B)}} \sin\delta_W \tag{6A}$$

for the forward lifting surface and as

$$C_{A_{\delta_T}} = (C_{N_{T(B)}} + C_{N_{T(V)}}) \sin\delta_T \tag{6B}$$

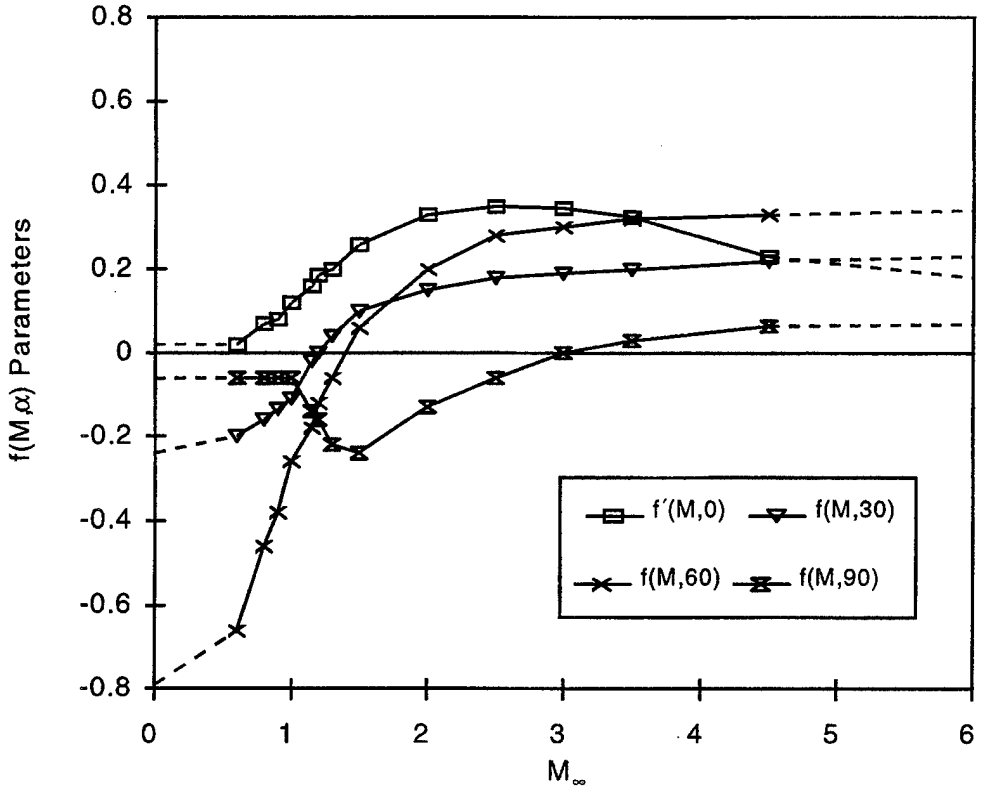

FIGURE 2. AXIAL FORCE AOA VARIATION PARAMETERS FOR A BODY-TAIL CONFIGURATION

for a rearward lifting surface if two sets of lifting surfaces are present. If only one set of lifting surfaces are present, Equation (6A) applies regardless of the fin location. Equation (6B) contains the tail interference term as a result of the forward set of fins, whereas Equation (6A) does not have this term. Both $C_{N_{W(B)}}$ and $C_{N_{T(B)}}$ of Equation (6) are the normal force coefficient on the wing or tail due to both AOA and control deflection.

In analyzing Equations (6A) and (6B), they both basically assume that the axial force due to control deflection is simply the normal force of the wing in conjunction with the body times the sine of the control deflection angle δ. In examining comparisons of this approach to data, it was found that when α and δ were of the same sign, Equation (6) gave agreement with experimental data which was quite acceptable. However, when α and δ were of opposite signs, it was found the agreement was not as good for higher Mach numbers. It is suspected that part of the reason for this is the nonlinear model of $k_{W(B)}$ and $k_{B(W)}$ are accurate for α and δ of the same sign, but when α and δ are of opposite signs, the total values of $k_{W(B)}$ and $k_{B(W)}$ are correct, but each may be in error and the errors tend to compensate. It is speculated that the fundamental source of this discrepancy is wing gap effects when the wings are deflected. This cancellation of errors could give accurate normal force, but possibly inaccurate axial force contributions due to AOA. The other possible source of the inaccuracy in the C_{A_α} term is the fact that $k_{W(B)}$ does not include nonlinearities from control deflection (only α, M, AR, λ nonlinearities are included). These nonlinear wing gap effects could be accounted for adequately when α and δ are of the same sign from the α alone contribution, but inadequately when they are of opposite sign.

TABLE 2. VALUES OF THE AXIAL FORCE AOA PARAMETERS FOR A BODY-TAIL CONFIGURATION

M	f'(M,0)	f(M,30)	f(M,60)	f(M,90)
0	0.020	-0.240	-0.79	-0.060
0.6	0.020	-0.200	-0.66	-0.060
0.8	0.070	-0.160	-0.46	-0.060
0.9	0.080	-0.135	-0.38	-0.060
1.0	0.120	-0.110	-0.26	-0.060
1.15	0.160	-0.020	-0.18	-0.140
1.2	0.186	0	-0.12	-0.160
1.3	0.200	0.040	-0.06	-0.220
1.5	0.258	0.100	0.06	-0.240
2.0	0.330	0.150	0.20	-0.130
2.5	0.350	0.180	0.28	-0.060
3.0	0.346	0.190	0.30	0
3.5	0.325	0.200	0.32	0.030
4.5	0.230	0.220	0.33	0.065
≥6.0	0.180	0.230	0.34	0.070

Since no direct data measurements are available and since the control deflection matrix of Reference 1 gives quite acceptable values of normal force and pitching moment, the approach taken here is to define a term $f(M,\alpha_W)$ to multiply Equation (6) by when α and δ are of opposite signs.

Then

$$C_{A_{\delta_W}} = (C_{N_{W(B)}} \sin\delta_W)\ f(M,\alpha_W) \tag{7A}$$

and

$$C_{A_{\delta_T}} = (C_{N_{T(B)}} + C_{N_{T(V)}})\ \sin\delta_T\ f(M,\alpha_T) \tag{7B}$$

α_W and α_T of Equations (7) are defined by

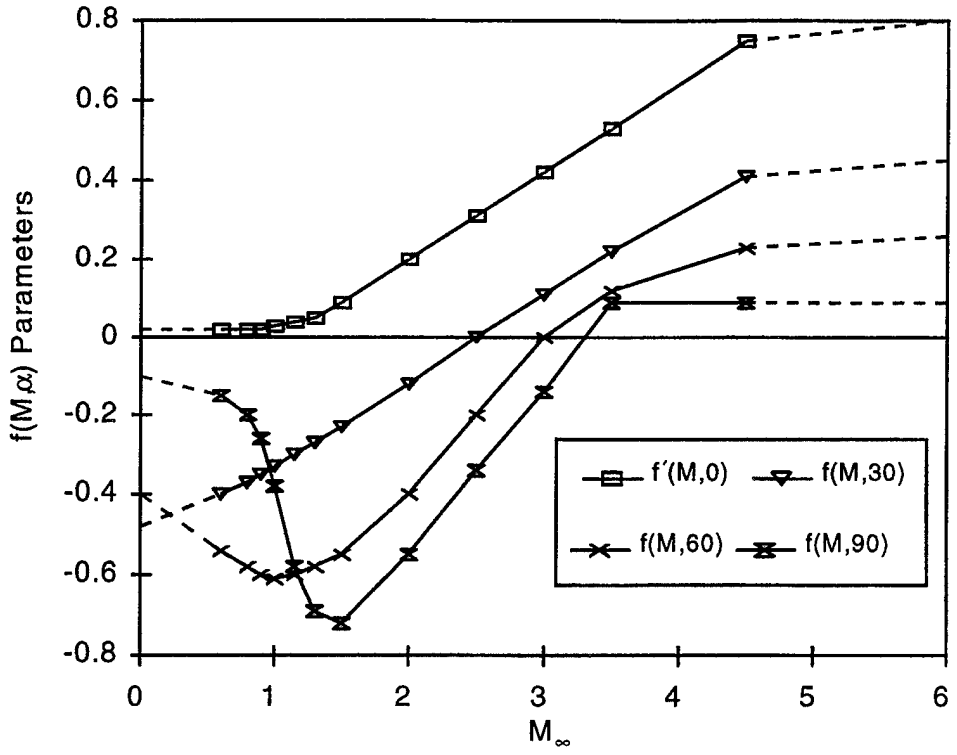

FIGURE 3. AXIAL FORCE AOA VARIATION PARAMETERS FOR A WING-BODY-TAIL CONFIGURATION

$$\alpha_W = \alpha + \delta_W$$
$$\alpha_T = \alpha + \delta_T \qquad (8)$$

Since the generic wind tunnel data bases available have fins that are too small to accurately determine f(M, α), use of other data bases[18,21] in conjunction with the AP95 code will be used instead. Figure 4A and Table 4A give values of f(M,α_W) for Mach numbers between 1.5 and 4.60 at $\Phi = 0$, and Figure 4B and Table 4B give the complementary values at $\Phi = 45$ deg. For Mach numbers above 4.6, the values at 4.6 are used. For Mach numbers below 1.5, f(M,α_W) is assumed to go to its value of 1.0 at $M_\infty = 0.8$ and remain at that value below that Mach number. This assumption again is based on comparisons to data at low speeds. For α and δ of the same sign, f(M,α_W) is always 1.0.

It should also be pointed out that the value of f(M,α_W) at $\alpha_W = 90$ deg has been assumed to be 0.5 for both the $\Phi = 0$ and $\Phi = 45$ deg planes. If the wing were not in the presence of the body, then a value of 1.0 would be natural at least at $\Phi = 0$. However, due to body interference, the full effect of control deflection on f(M,α_W) at α_W does not appear to be obtained at $\alpha_W = 90$ deg based on extrapolated experimental data at lower values of α_W. Hence, the assumed value of 0.5. Hopefully, higher AOA experimental data will become available that can be used to improve upon this assumption.

TABLE 3. VALUES OF THE AXIAL FORCE AOA PARAMETERS FOR A WING-BODY-TAIL CONFIGURATION

M	f'(M,0)/rad	f(M,30)	f(M,60)	f(M,90)
0	0.02	-0.48	-0.40	-0.10
0.60	0.02	-0.40	-0.54	-0.15
0.80	0.02	-0.37	-0.58	-0.20
0.90	0.02	-0.35	-0.60	-0.26
1.00	0.03	-0.33	-0.61	-0.38
1.15	0.04	-0.30	-0.60	-0.58
1.30	0.05	-0.27	-0.58	-0.69
1.50	0.09	-0.23	-0.55	-0.72
2.00	0.20	-0.12	-0.40	-0.55
2.50	0.31	0	-0.20	-0.34
3.00	0.42	0.11	0	-0.14
3.50	0.53	0.22	0.12	-0.09
4.50	0.75	0.41	0.23	-0.09
≥6.00	0.80	0.45	0.26	-0.09

Where $C_A(M,90) = C_A(M,0) + f(M,90) \geq 0$

The final issue that must be resolved is how to break down the changes in C_A with AOA into the individual components. The AP95[1] currently breaks these components down into those due to axial pressure drag, skin-friction and base drag. The present AP95 methodology uses the work of Reference 13 to account for changes in C_A to AOA 30 deg. From AOA 30 to 90 deg, C_{A_B} is assumed to go linearly to zero from its value at AOA 30 deg. The approach to compute C_{A_B} will not change from Reference 1 since Reference 1 was based on wind tunnel data. It will be assumed that C_{A_f} is independent of AOA. This means that the remaining change in C_A with AOA is accounted for in the pressure term. Thus

$$(\Delta C_{A_p})_\alpha = f(M,\alpha) - (\Delta C_{A_B})_\alpha \tag{9}$$

Then, the individual components of axial force of the body are

$$(C_{A_p})_\alpha = (C_{A_p})_{\alpha=0} + (\Delta C_{A_p})_\alpha \tag{10A}$$

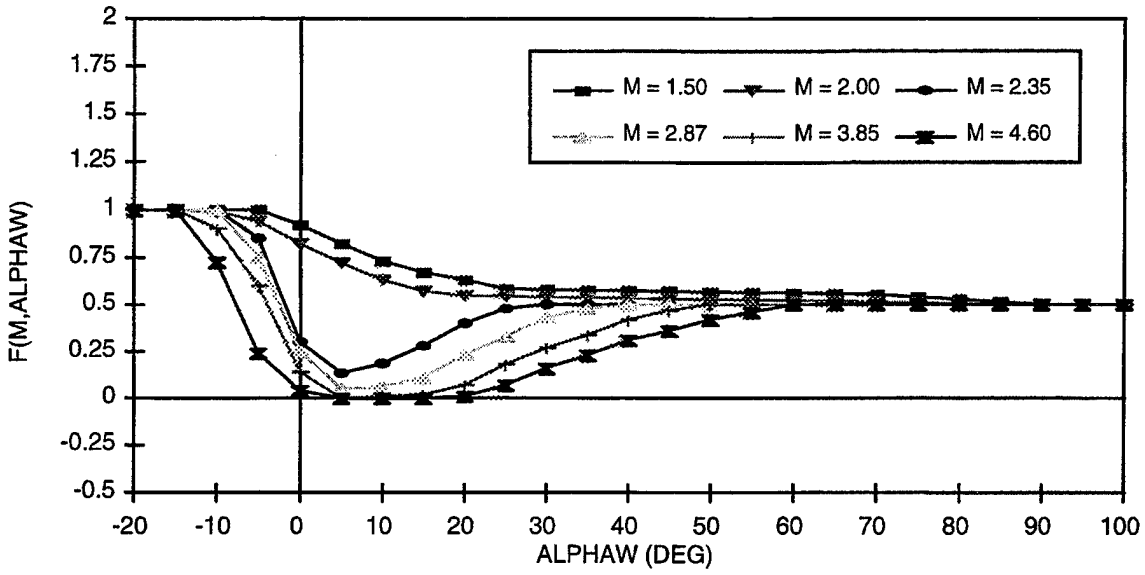

(A) $\Phi = 0$ deg

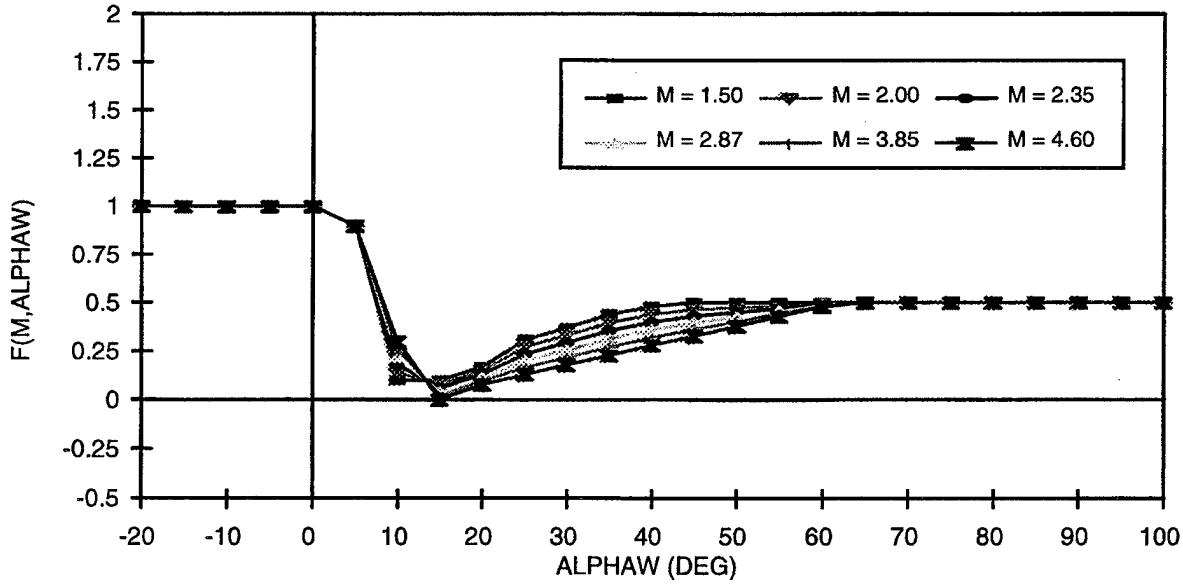

(B) $\Phi = 45$ deg

FIGURE 4. $f(M,\alpha_w)$ VALUES FOR α AND δ OF OPPOSITE SIGNS

TABLE 4A. $f(M,\alpha_W)$ AT $\Phi = 0$ deg

α_W	M = 1.50	M = 2.00	M = 2.35	M = 2.87	M = 3.85	M = 4.60
-20.0	1.0000	1.0000	1.0000	1.0000	1.0000	1.0000
-15.0	1.0000	1.0000	1.0000	1.0000	1.0000	1.0000
-10.0	1.0000	0.9900	1.0000	1.0000	0.9000	0.7232
-5.0	1.0000	0.9400	0.8500	0.7500	0.6000	0.2400
0.0	0.9200	0.8200	0.3000	0.2500	0.1400	0.4000
5.0	0.8200	0.7200	0.1328	0.0500	0.0000	0.0000
10.0	0.7300	0.6300	0.1833	0.0597	0.0100	0.0000
15.0	0.6700	0.5700	0.2800	0.1100	0.0200	0.0000
20.0	0.6300	0.5470	0.4000	0.2300	0.0700	0.0100
25.0	0.5836	0.5436	0.4800	0.3300	0.1800	0.0700
30.0	0.5803	0.5403	0.5000	0.4300	0.2700	0.1600
35.0	0.5769	0.5369	0.5000	0.4800	0.3400	0.2300
40.0	0.5736	0.5336	0.5000	0.5000	0.4200	0.3100
45.0	0.5702	0.5302	0.5000	0.5000	0.4700	0.3600
50.0	0.5669	0.5269	0.5000	0.5000	0.5000	0.4200
55.0	0.5635	0.5235	0.5000	0.5000	0.5000	0.4600
60.0	0.5602	0.5202	0.5000	0.5000	0.5000	0.5000
65.0	0.5568	0.5168	0.5000	0.5000	0.5000	0.5000
70.0	0.5535	0.5135	0.5000	0.5000	0.5000	0.5000
75.0	0.5401	0.5101	0.5000	0.5000	0.5000	0.5000
80.0	0.5268	0.5068	0.5000	0.5000	0.5000	0.5000
85.0	0.5134	0.5034	0.5000	0.5000	0.5000	0.5000
90.0	0.5000	0.5000	0.5000	0.5000	0.5000	0.5000
95.0	0.5000	0.5000	0.5000	0.5000	0.5000	0.5000
100.0	0.5000	0.5000	0.5000	0.5000	0.5000	0.5000

TABLE 4B. $f(M,\alpha_w)$ AT $\Phi = 45$ deg

α_w	M = 1.50	M = 2.00	M = 2.35	M = 2.87	M = 3.85	M = 4.60
-20.0	1.0000	1.0000	1.0000	1.0000	1.0000	1.0000
-15.0	1.0000	1.0000	1.0000	1.0000	1.0000	1.0000
-10.0	1.0000	1.0000	1.0000	1.0000	1.0000	1.0000
-5.0	1.0000	1.0000	1.0000	1.0000	1.0000	1.0000
0.0	1.0000	1.0000	1.0000	1.0000	1.0000	1.0000
5.0	0.9000	0.9000	0.9000	0.9000	0.9000	0.9000
10.0	0.1000	0.1400	0.1800	0.2200	0.2600	0.3000
15.0	0.1000	0.0800	0.0600	0.0400	0.0200	0.0000
20.0	0.1700	0.1520	0.1340	0.1160	0.0980	0.0800
25.0	0.3100	0.2740	0.2380	0.2020	0.1660	0.1300
30.0	0.3700	0.3320	0.2940	0.2560	0.2180	0.1800
35.0	0.4400	0.3980	0.3560	0.3140	0.2720	0.2300
40.0	0.4800	0.4400	0.4000	0.3600	0.3200	0.2800
45.0	0.5000	0.4660	0.4320	0.3980	0.3640	0.3300
50.0	0.5000	0.4760	0.4520	0.4280	0.4040	0.3800
55.0	0.5000	0.4860	0.4720	0.4580	0.4440	0.4300
60.0	0.5000	0.4960	0.4920	0.4880	0.4840	0.4800
65.0	0.5000	0.5000	0.5000	0.5000	0.5000	0.5000
70.0	0.5000	0.5000	0.5000	0.5000	0.5000	0.5000
75.0	0.5000	0.5000	0.5000	0.5000	0.5000	0.5000
80.0	0.5000	0.5000	0.5000	0.5000	0.5000	0.5000
85.0	0.5000	0.5000	0.5000	0.5000	0.5000	0.5000
90.0	0.5000	0.5000	0.5000	0.5000	0.5000	0.5000
95.0	0.5000	0.5000	0.5000	0.5000	0.5000	0.5000
100.0	0.5000	0.5000	0.5000	0.5000	0.5000	0.5000

$$(C_{A_f})_\alpha = (C_{A_f})_{\alpha=0} \tag{10B}$$

$$(C_{A_B})_\alpha = (C_{A_B})_{\alpha=0} + (\Delta C_{A_B})_\alpha \tag{10C}$$

Of course,

$$(C_A)_\alpha = (C_{A_P})_\alpha + (C_{A_f})_\alpha + (C_{A_B})_\alpha = C_{A_O} + f(M,\alpha) \tag{11}$$

It will also be assumed that there is no change in the zero lift axial force coefficient of a lifting surface with AOA. This assumption will also apply to the components of axial force on the lifting surface. Thus all the axial force change with AOA for bodies alone or those with lifting surfaces at $\delta = 0$ will be accounted for by the body change in C_A with AOA. These changes are defined by Equations (9) through (11). The lifting surface change in C_A due to δ is accounted for by Equation (7) with $f(M,\alpha_W)$ being 1.0 when α and δ are the same sign and varying according to Table 4 when of opposite signs.

3.0 RESULTS AND DISCUSSION

The first case to compare the new axial force methodology to experimental data is the large NASA/Tri-Service[14] wind tunnel data base. Body alone wind tunnel results are compared to the new theory at Mach numbers 0.6 to 4.5. The wind tunnel model tested was 12.33 calibers long with a 3.0 caliber tangent ogive nose (see Figure 5A). It had a boundary layer trip and was tested at Reynolds numbers of about 2×10^6/ft for most conditions. Thus the "wind tunnel model with boundary layer trip" option was used in the aeroprediction code to compute the skin-friction component of axial force. This option means that flow is assumed to be turbulent over the entire body. The wind tunnel data were given in terms of forebody and chamber axial force. These two values were added together to compare against the total aeroprediction axial force predictions. It is suspected that at subsonic Mach numbers, the chamber axial force is somewhat different than the base drag with a solid base. Hopefully, the AOA corrections will be similar for the two, however.

Figure 5B presents the results of the comparison between the aeroprediction axial force and those from wind tunnel results for the body alone case of Figure 5A. The wind tunnel data were only available to 30 deg AOA at lower Mach numbers, but up to 45 deg AOA at high Mach numbers. As seen in the figure, the new method is superior to that in the AP95, particularly above AOA 30 deg. It is also seen that at the higher Mach numbers C_{A_O} as well as C_{A_α} are both predicted reasonably well, whereas at the lower Mach numbers, C_{A_α} has the right trend but total C_A differs from the data

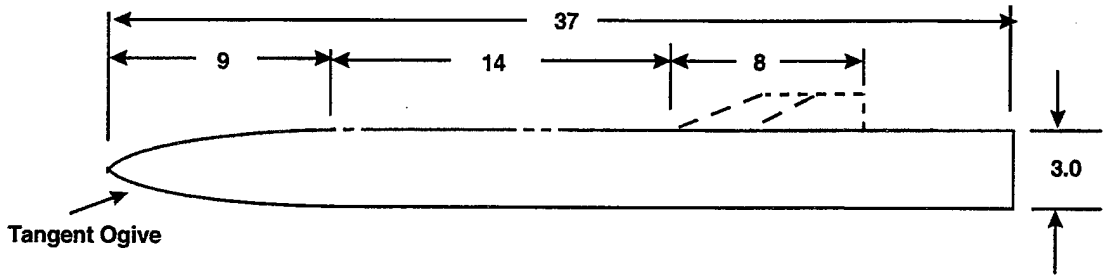

Body Alone with Tail Location

(All Dimensions in Inches)

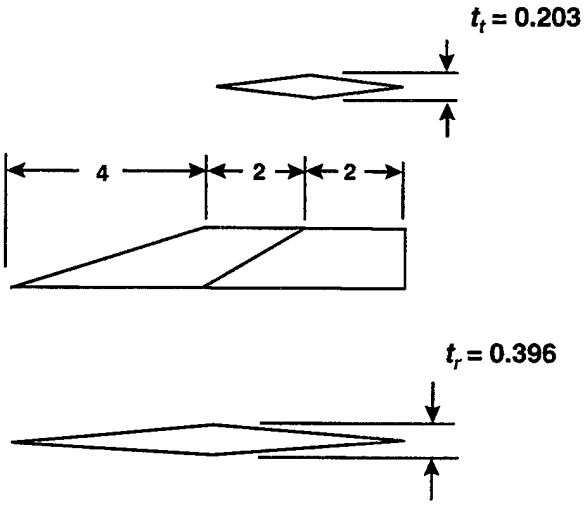

Tail Planform and Cross-Section Shape

FIGURE 5A. BODY ALONE AND ONE BODY-TAIL CONFIGURATION OF NASA TRI-SERVICE DATA BASE[14]

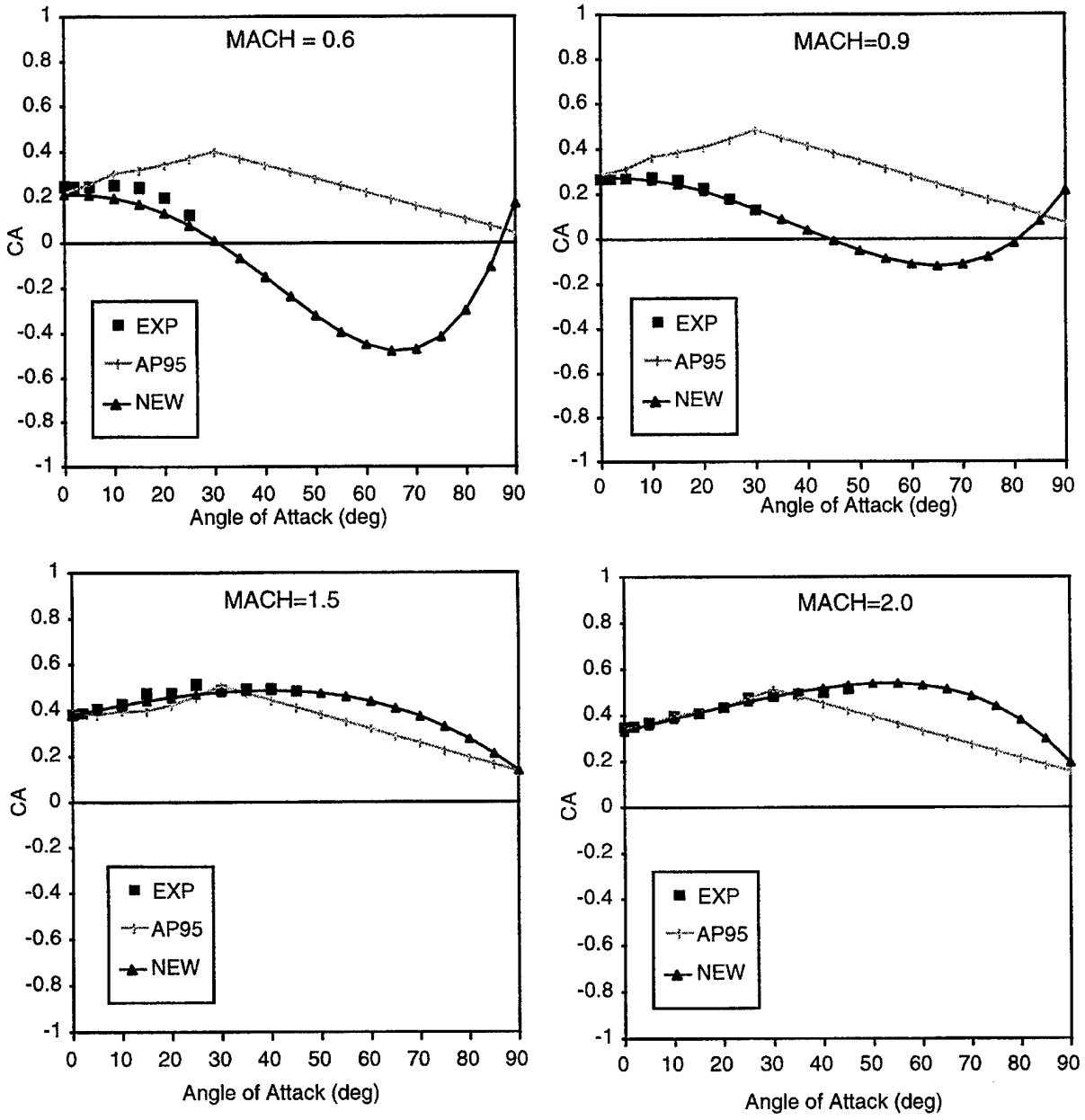

FIGURE 5B. COMPARISON OF AXIAL FORCE COEFFICIENTS OF THEORY AND EXPERIMENT FOR NASA BODY ALONE CONFIGURATION OF FIGURE 5A

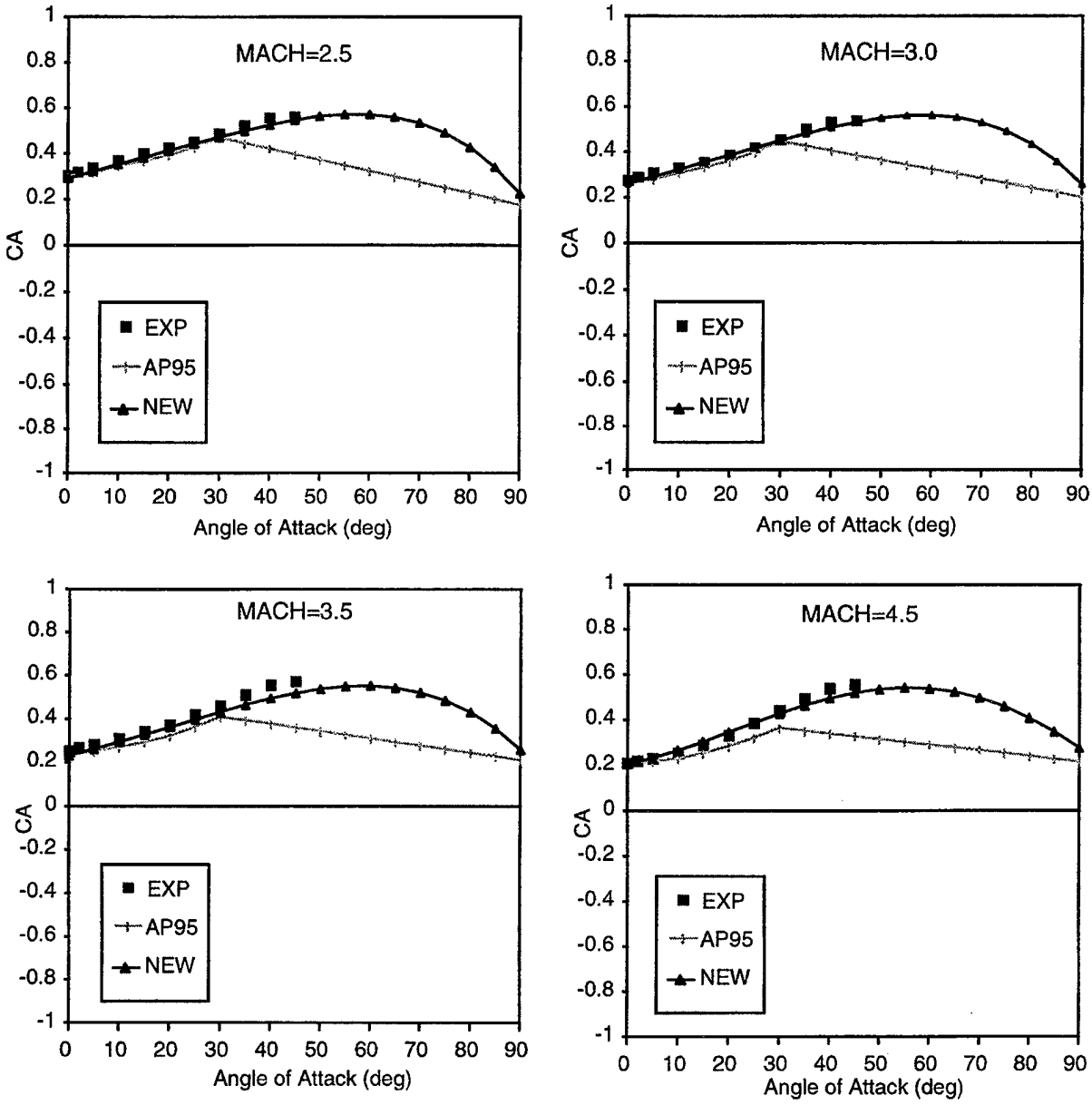

FIGURE 5B. COMPARISON OF AXIAL FORCE COEFFICIENTS OF THEORY AND EXPERIMENT FOR NASA BODY ALONE CONFIGURATION OF FIGURE 5A (CONTINUED)

due to C_{A_0}. It is believed the theoretical predictions are closer to actual fight conditions than the model due to the fact that the model had a large hollow chamber and the prediction assumed a solid base. The base drag for a configuration like this with a solid base at subsonic Mach numbers is about 0.12. This is almost as large as the total experimental axial force given in Figure 5B for $M_\infty = 0.6$ and 0.9. Hence, in viewing the comparisons with data, one should keep this fact in mind.

The body-tail configuration (Figure 5A) comparisons of experiment[14] and the new method are given in Figure 5C for the basic same wind tunnel parameters as for Figure 5B. That is, a configuration with a boundary layer trip tested at R_N/ft of 2×10^6. Mach numbers shown in Figure 5C vary from 0.6 to 4.5. Figure 5B utilized Table 1 and Figure 1 in the new methodology, whereas Figure 5C uses Figure 2 and Table 2. As seen in the various comparisons of C_A as a function of AOA for various Mach numbers, the improved AOA theory gives much better agreement to data than the AP95 results. It is also seen that the average accuracy goal of ±10 percent on C_A is easily obtained with the new theory, whereas the AP95 did not achieve this goal at higher AOA.

The third case considered is one of the body alone configurations tested by Baker.[15] The Baker data base was the primary data base upon which the theoretical axial force methods of References 3 through 5 were based. This data base consisted of several body alone and body-tail configurations tested at AOAs to 180 deg and Mach numbers 0.6 to 3.0. Figure 6A shows the body alone and body-tail considered as an example here. The body has a 2.5 caliber tangent ogive nose and 7.5 caliber cylindrical afterbody. The tail planform has an aspect ratio of one. The configuration was tested with a boundary layer trip at a Reynolds number of 4×10^6/ft.

Figure 6B compares the new theoretical approach with the body alone axial force data of Reference 15. Also shown on Figure 6B for the lower Mach number cases is the fourth order axial force method of Reference 4 and the third order method of Reference 5 for the higher Mach number cases. Note that the new method achieves one of its objectives of being as accurate as the References 4 and 5 methods, while using a single versus dual methods. One of the reasons References 4 and 5 methods compare as well as they do to data is the C_{A_0} prediction that is based on the Baker data base. The new method uses AP95 theoretical methodology to predict C_{A_0} and still gives as good or better comparison to the Baker[15] data than either Reference 3 or 4.

Figure 6C compares the predictions of the new theory to the Baker data and the methods of Ingram[5] and Jorgensen[2] at several supersonic Mach numbers for the body-tail configuration of Figure 6A. For the Jorgensen method, the AP95 value of C_{A_0} has been assumed. Note that both the third order[5] and the present fourth order in AOA methods predict C_{A_α} quite well for supersonic Mach numbers. However, the third order AOA method does not work well at subsonic Mach numbers. The Figure 6A configuration was tested with a boundary layer trip and a solid base so none of the chamber effects on base pressure are present as was the case with the NASA data base of Figure 5.

In examining the comparisons of the new method of this report to those of References 3 through 5 in Figures 5 and 6, it is seen that one of the objectives of this work has been achieved. That is, a single method (versus multiple methods) has been defined that works as well as or better than those available[3-5] for body alone and body-tail configurations over the entire Mach number range and for AOAs to 90 deg. The method has been validated for a more limited Mach number range due to availability of data however.

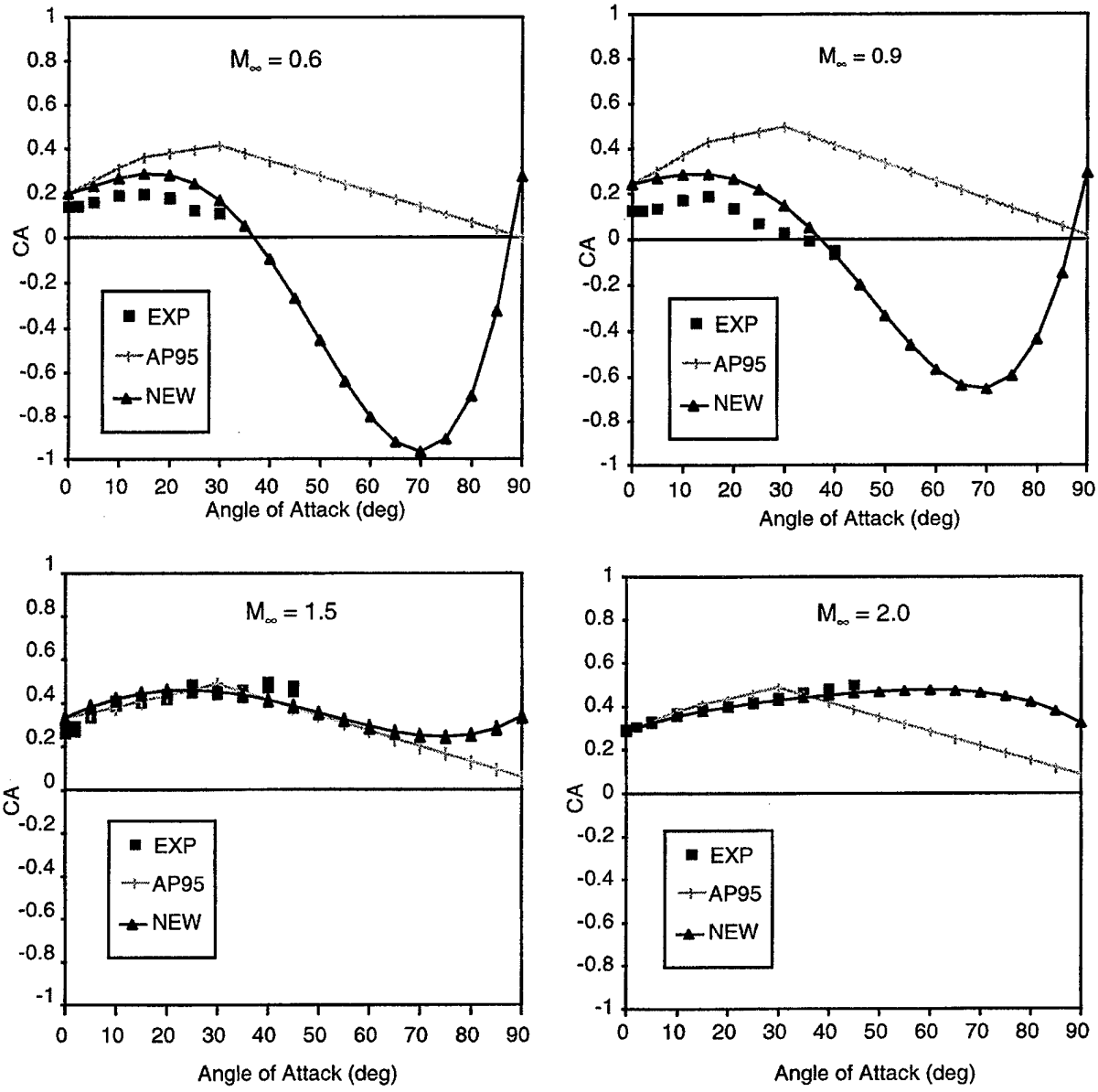

FIGURE 5C. COMPARISON OF AXIAL FORCE COEFFICIENTS OF THEORY AND EXPERIMENT FOR NASA BODY-TAIL CONFIGURATION OF FIGURE 5A

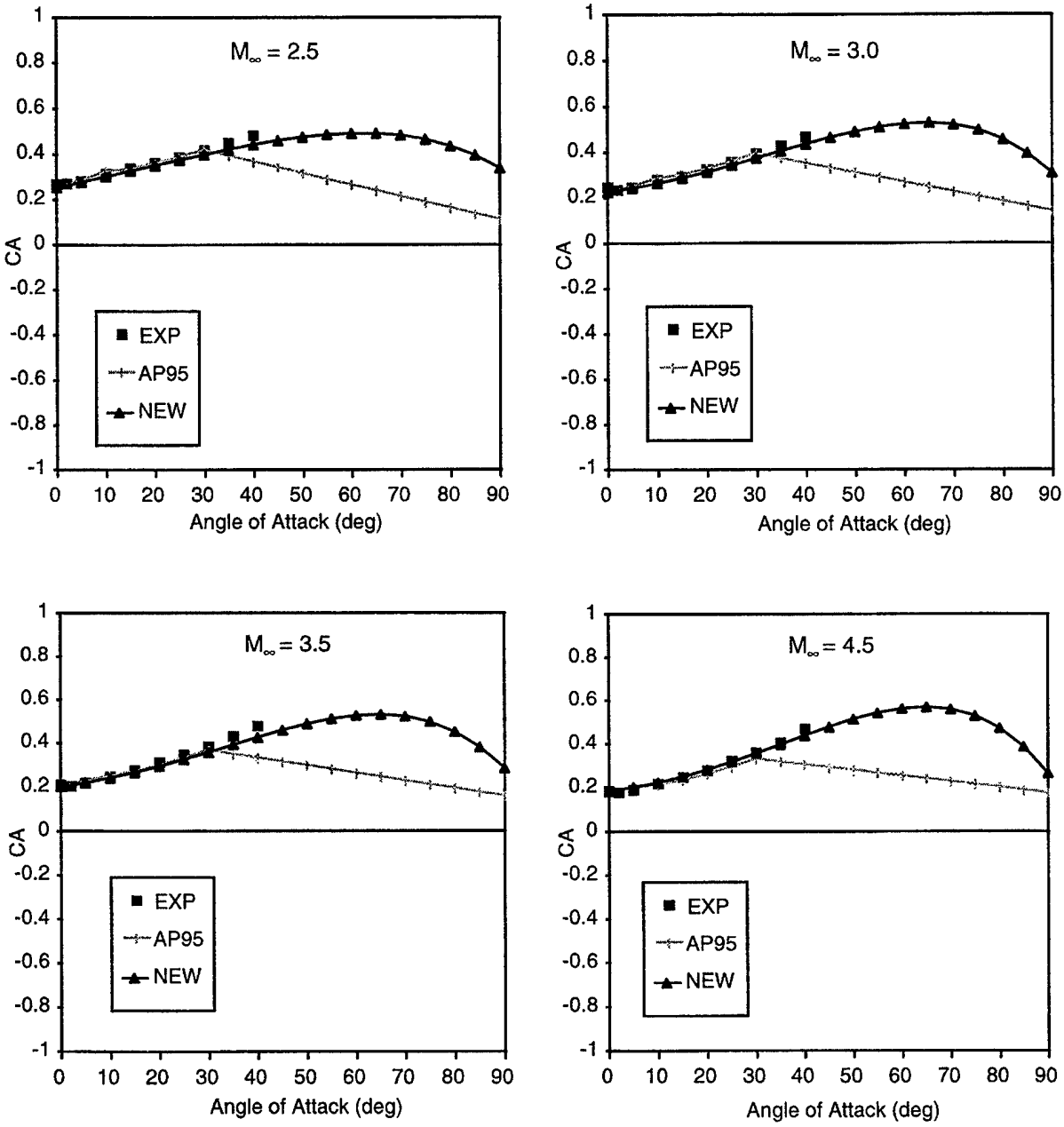

FIGURE 5C. COMPARISON OF AXIAL FORCE COEFFICIENTS OF THEORY AND EXPERIMENT FOR NASA BODY-TAIL CONFIGURATION OF FIGURE 5A (CONTINUED)

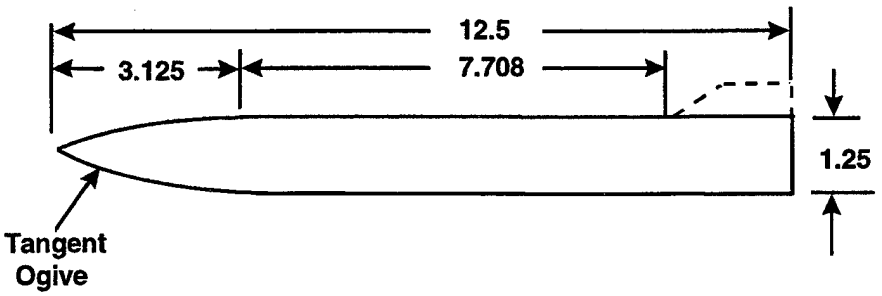

Body Alone with Tail Location

All Dimensions in Inches

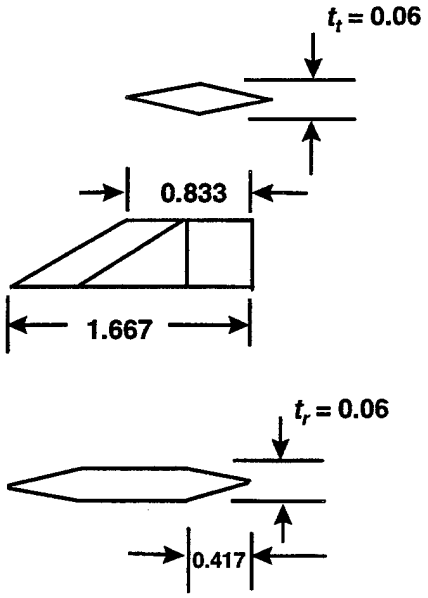

Tail Planform and Cross Section Shape

FIGURE 6A. BODY ALONE AND ONE BODY-TAIL CONFIGURATION OF BAKER DATA BASE[15]

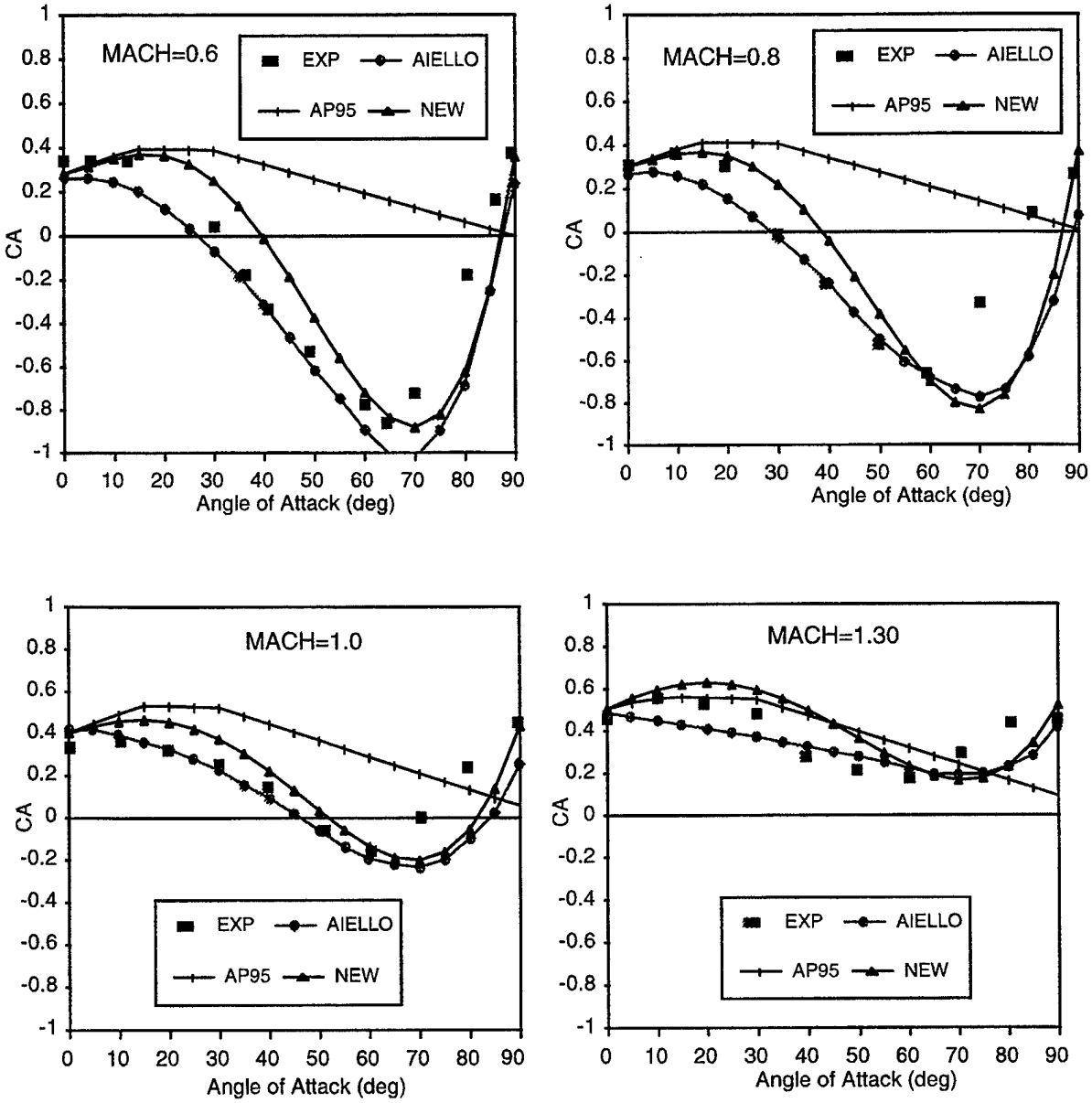

FIGURE 6B. COMPARISON OF AXIAL FORCE COEFFICIENTS OF THEORY AND EXPERIMENT[15] FOR BODY ALONE OF FIGURE 6A

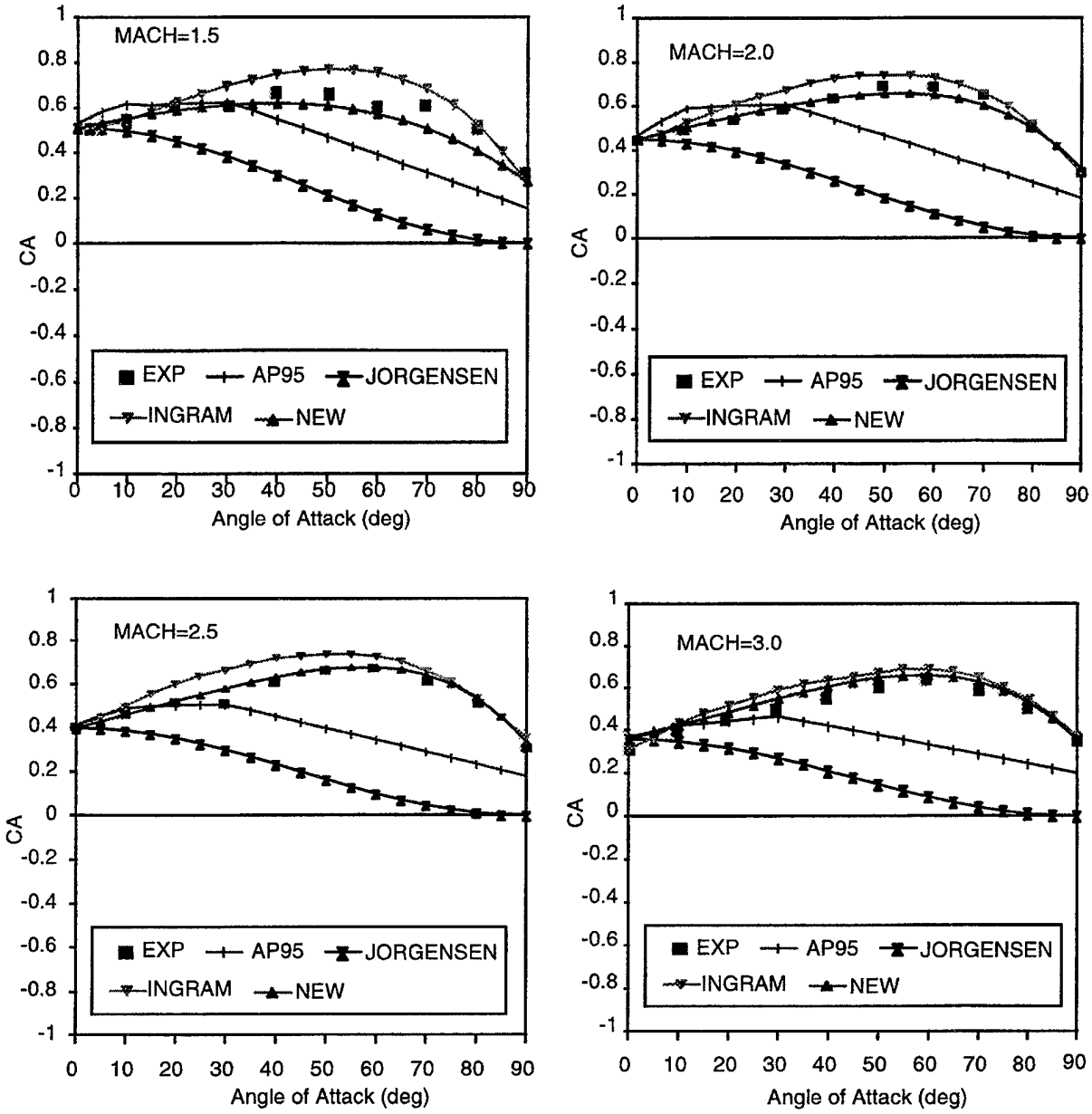

FIGURE 6B. COMPARISON OF AXIAL FORCE COEFFICIENTS OF THEORY AND EXPERIMENT[15] FOR BODY ALONE OF FIGURE 6A (CONTINUED)

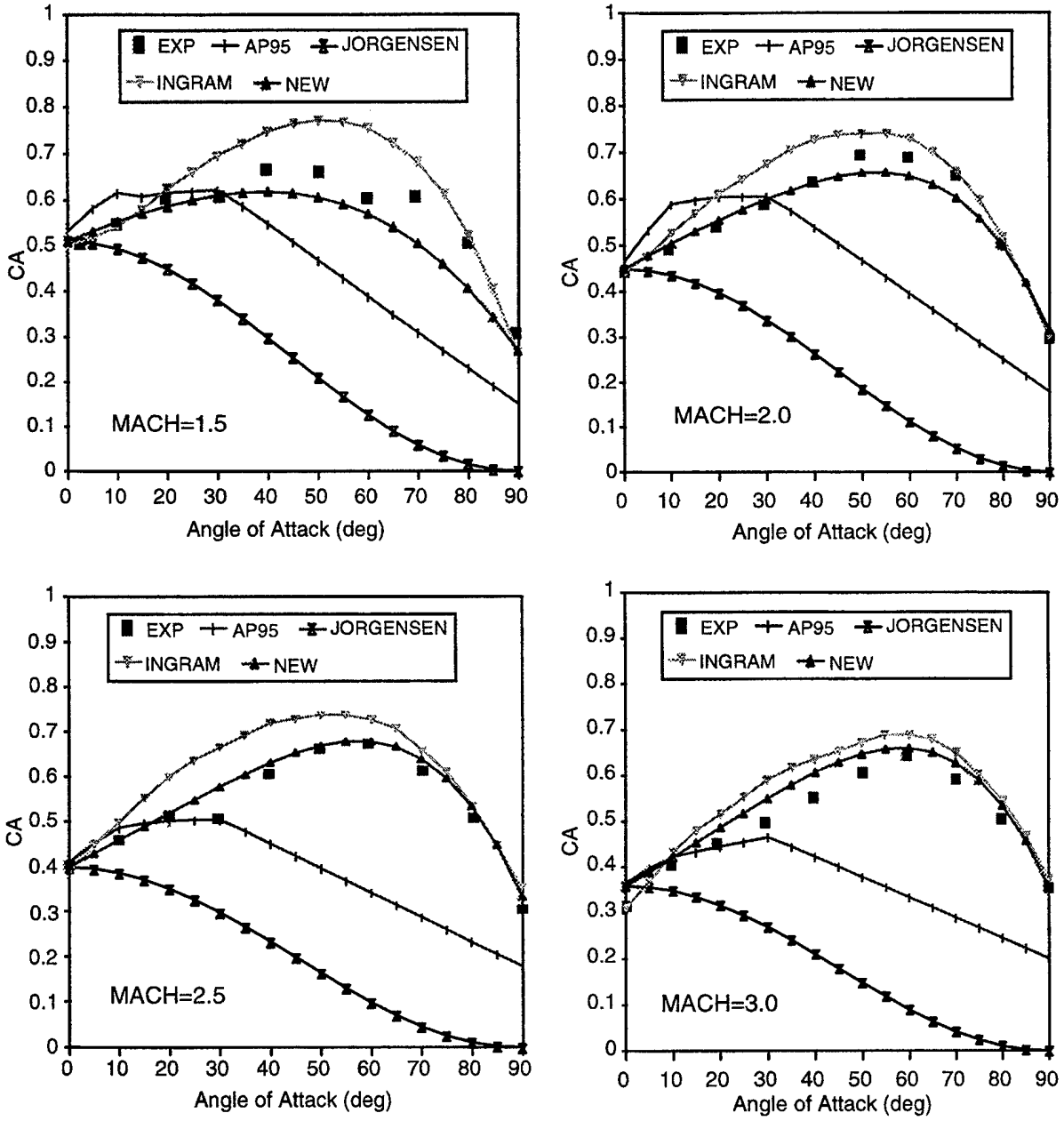

FIGURE 6C. COMPARISON OF AXIAL FORCE COEFFICIENTS OF THEORY AND EXPERIMENT[15] FOR BODY-TAIL CONFIGURATION OF FIGURE 6A

References 3 through 5 derived nonlinear AOA predictors for C_A for body alone and body-tail configurations. No consideration was given to configurations with more than one set of lifting surfaces or to control deflections so the user of this technology is left with the use of body-tail methodology for configurations with more than one set of lifting surfaces. The next several examples will apply the present new method of predicting C_{A_α} for configurations with more than one set of lifting surfaces. The theory for these examples is based on AP95 methods at AOA = 0, Equations (2) and (3), along with Figure 3 and Table 3.

The first of the configurations with two sets of lifting surfaces is a canard-body-tail configuration with a hemispherical nose as shown in Figure 7A. This configuration was tested[17] with a boundary layer trip at a Reynolds number of 2×10^6/ft. The Mach numbers considered were 0.2 to 4.63 and AOAs only up to 20 deg. This configuration should therefore provide a good test of the C_{A_0} methodology of the AP95 as well as a check on the initial trends of C_{A_α}. It is also outside the data base upon which Figure 3 and Table 3 were derived.

Figure 7B presents results of the new method compared to the data[17] and the AP95 for Mach numbers 0.2, 0.6, 1.0, 1.2, 1.75, 2.86, 3.95, and 4.63. The theoretical computations are shown for AOA to 90 deg even though data are given to only 20 deg AOA. In comparing the AP95 and new method to the data, it is seen that near ($\alpha = 0$, both methods give C_{A_0} results well within the desired ±10 percent average accuracy goal. This is quite encouraging in view of the fairly complex configuration of Figure 7A. However, as AOA is increased above 0 deg, the new method gives trends which in general are superior to those of AP95, particularly at the lower and higher Mach number cases of Figure 7B.

The next case considered is a canard controlled missile model tested at the Naval Postgraduate School in Monterey (See Figure 8A). The configuration tested was a 1/3 scale model which was 22.6 calibers in length. It had canards with aspect ratio of 1.59 and fairly large tail surfaces with an aspect ratio of 0.9. Wind tunnel results are given for AOA to 45 deg at $M_\infty = 0.2$; for both $\Phi = 0$ and 45 deg roll positions; and for canard deflections of 0, +20 deg and −20 deg. Reference 18 stated that the sting balance was based on normal loads and therefore the axial loads could have considerable error as a result. The theoretical results were calculated based on a boundary layer trip and no boundary layer trip for control deflection of 0 deg. When the forward controls were deflected, it was assumed that the flow would be turbulent over the body surface, so the boundary layer trip option in the aeroprediction code was used for these calculations. Freestream Reynolds number of 1.42×10^6/ft was assumed for the computations based on sea level conditions.

Figure 8B and 8C compares the AP95 and new method to the experimental results from Reference 18. Reference 18 also gave Missile Datcom[19] results at $\delta = 0$, and these results are also given on the figure. Figure 8B gives the $\Phi = 0$ deg results and Figure 8C gives the $\Phi = 45$ deg results. In examining the $\Phi = 0$ deg and $\delta = 0$ deg results first, it is seen that the results for no boundary layer trip appear to match the data better than with a trip present and that both the new method results (with or without a trip) are superior to the AP95 and Missile Datcom results. For $\Phi = 0$ and $\delta = \pm 20$ deg, the AP95 is slightly better for the $\delta = +20$ deg case and the new method is better for $\delta = -20$ deg.

For the $\Phi = 45$ deg roll and $\delta = 0$ deg case of Figure 8C, it is seen that the zero AOA axial force measurement agrees closer to the case with a boundary layer trip than no boundary layer trip.

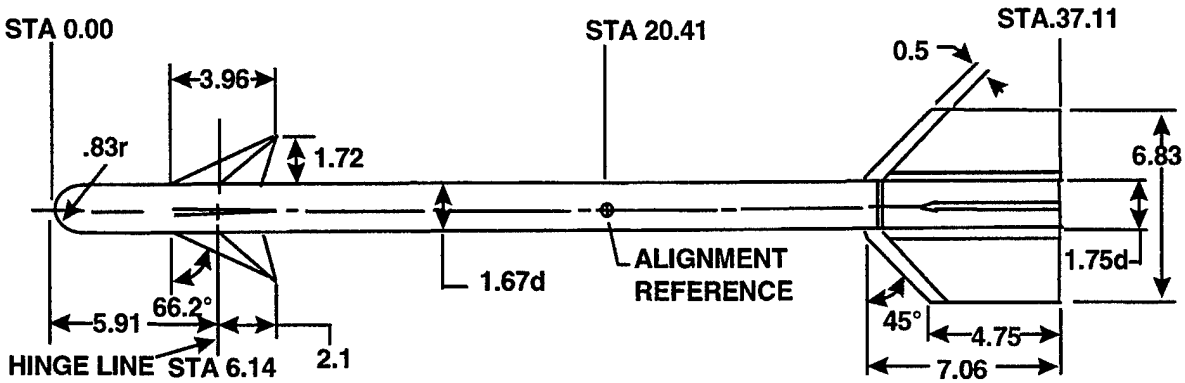

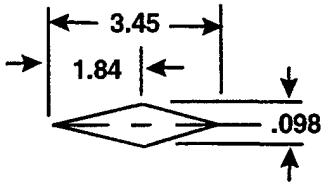

Canard Root
Chord Profile

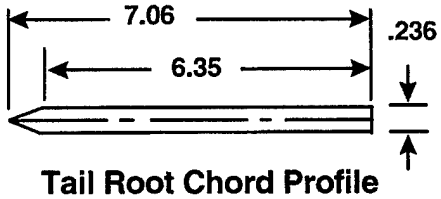

Tail Root Chord Profile

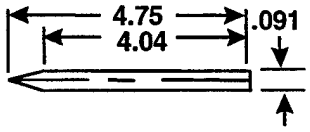

Tail Tip Chord Profile

FIGURE 7A. CANARD-BODY-TAIL CONFIGURATION WITH HEMISPHERICAL NOSE[17]

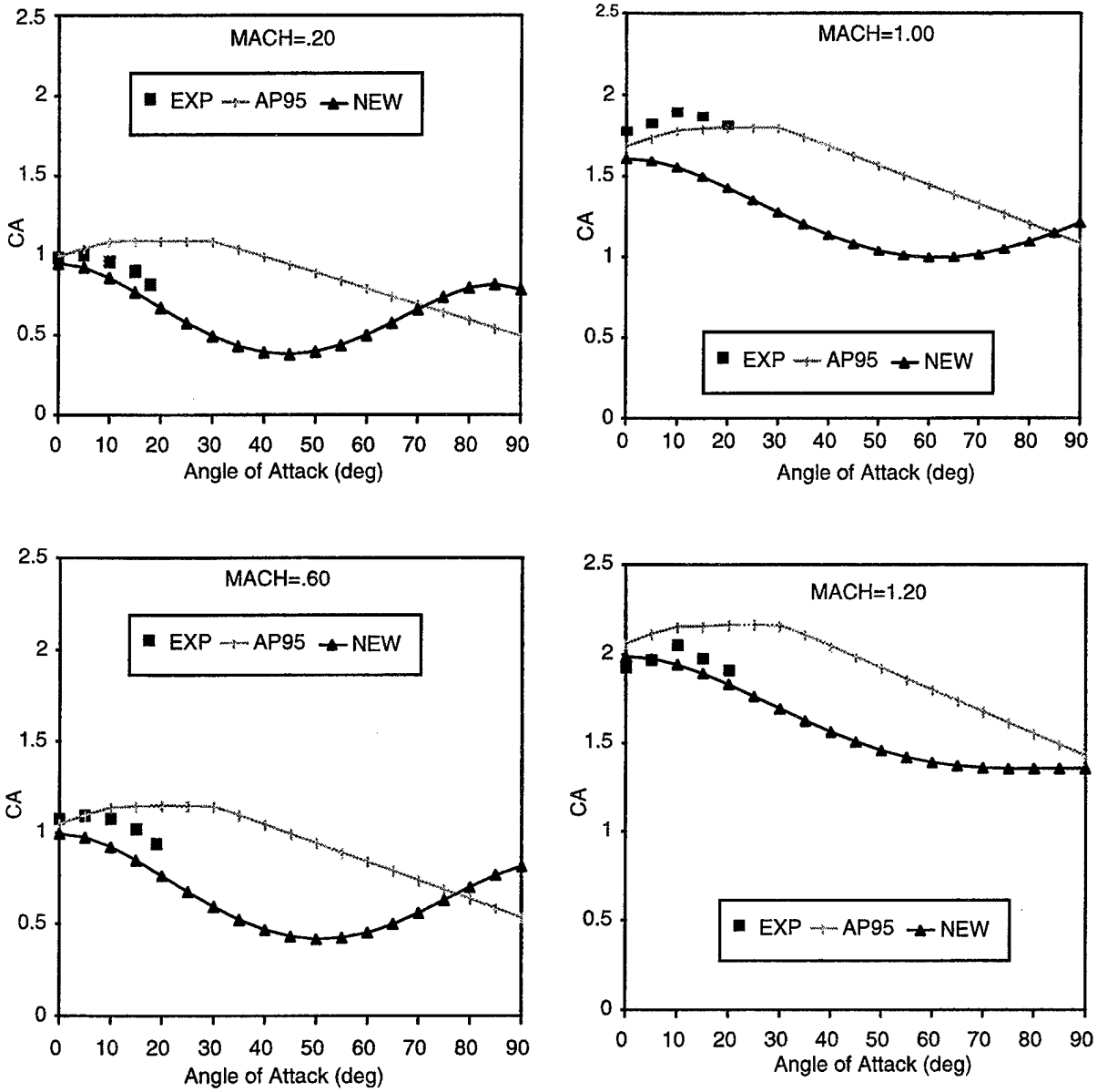

FIGURE 7B. AXIAL FORCE VERSUS AOA FOR THE CONFIGURATION OF FIGURE 7A

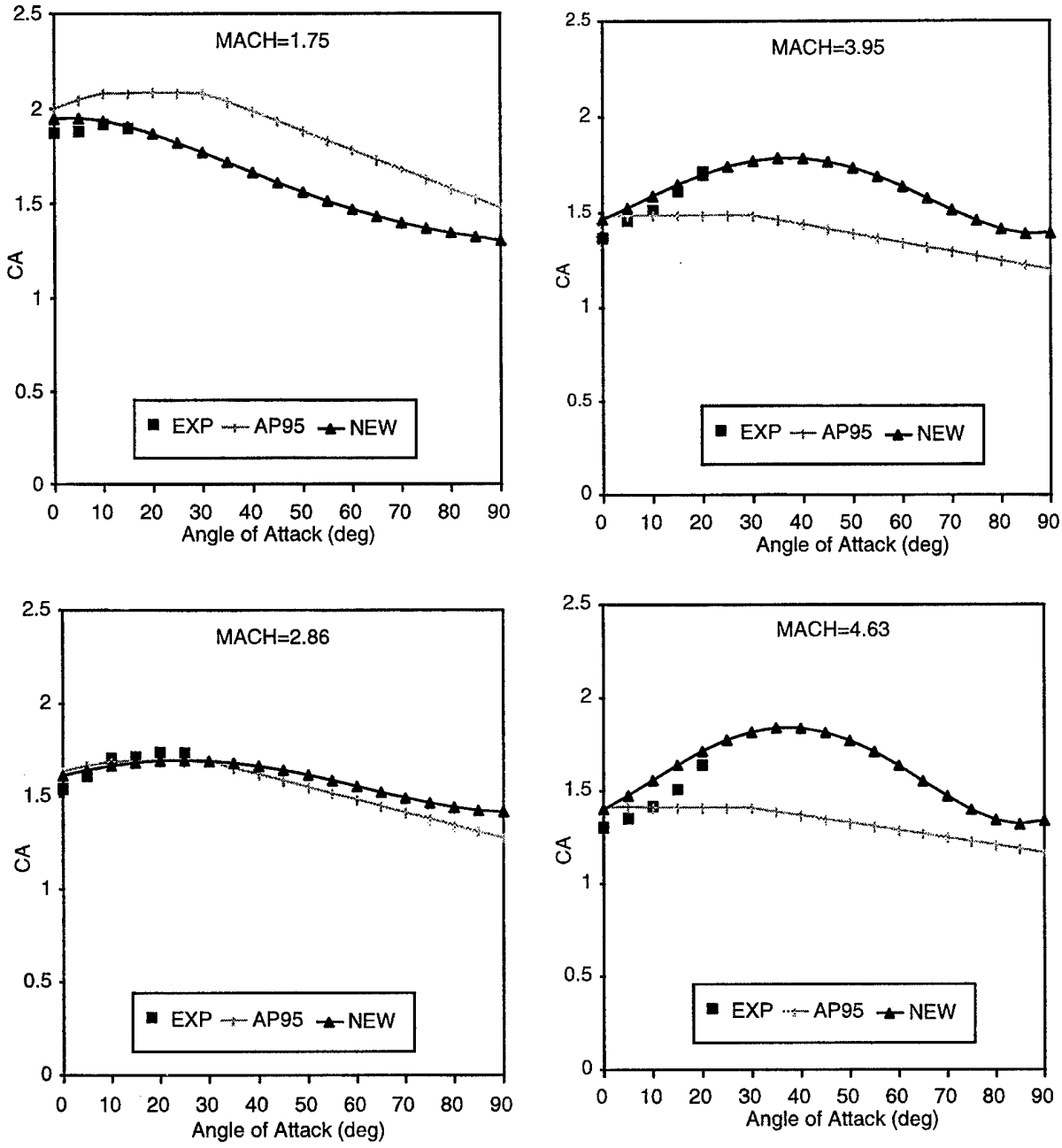

FIGURE 7B. AXIAL FORCE VERSUS AOA FOR THE CONFIGURATION OF FIGURE 7A (CONTINUED)

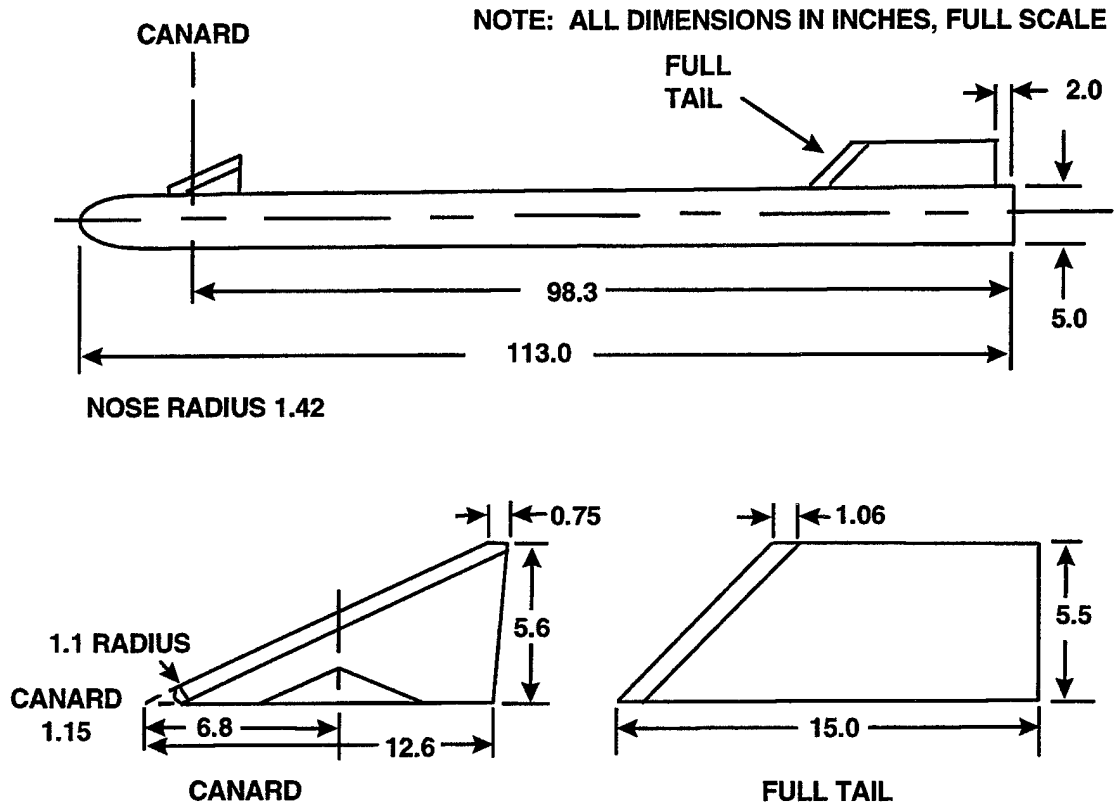

FIGURE 8A. CANARD-CONTROLLED MISSILE CONFIGURATION[18]
(WIND TUNNEL MODEL 1/3 SCALE)

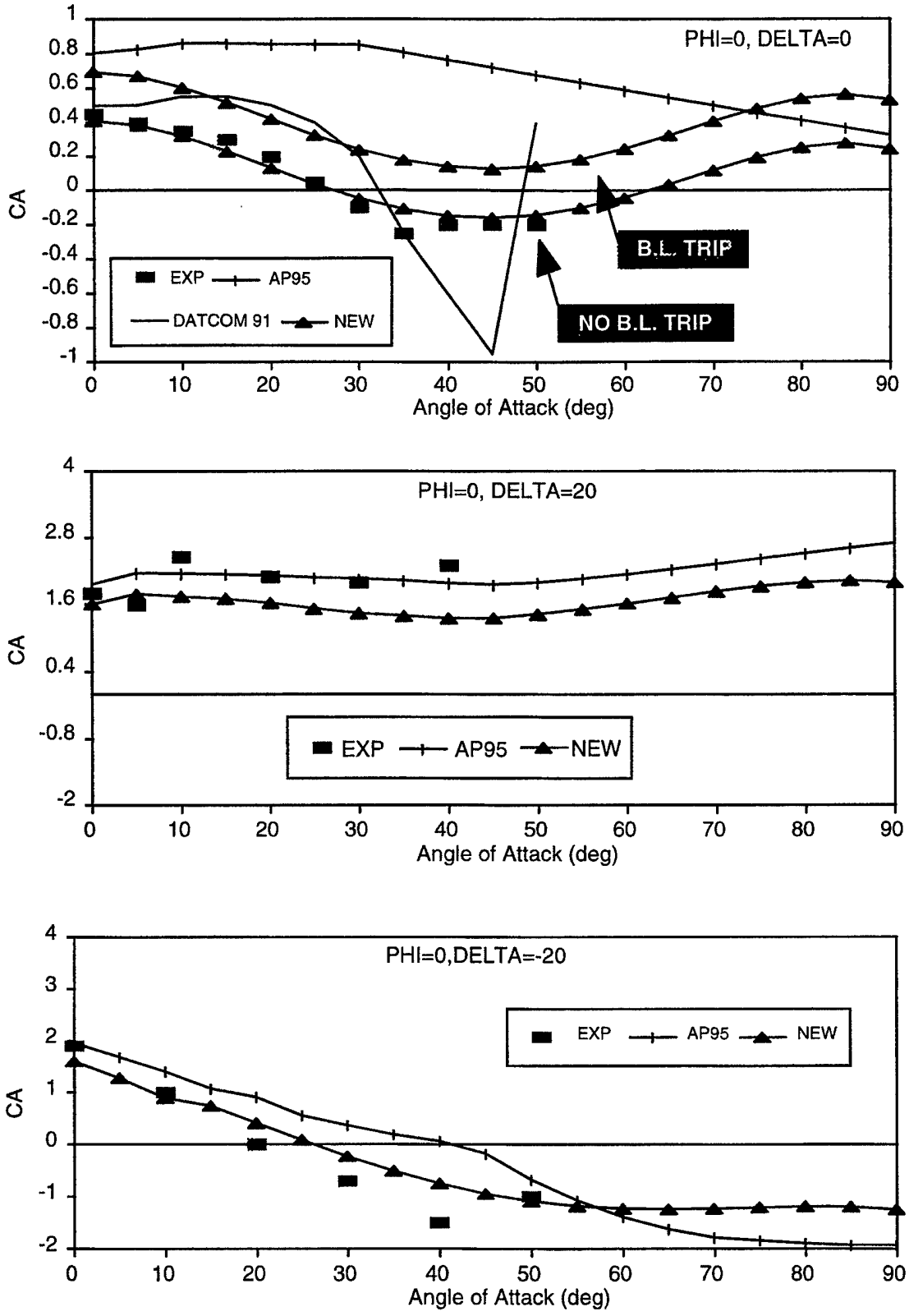

FIGURE 8B. COMPARISON OF THEORETICAL METHODS FOR AXIAL FORCE PREDICTION TO EXPERIMENT ON FIGURE 8A CONFIGURATION (Φ = 0 deg, M = 0.2, $R_N = 1.42 \times 10^{-6}$/ft)

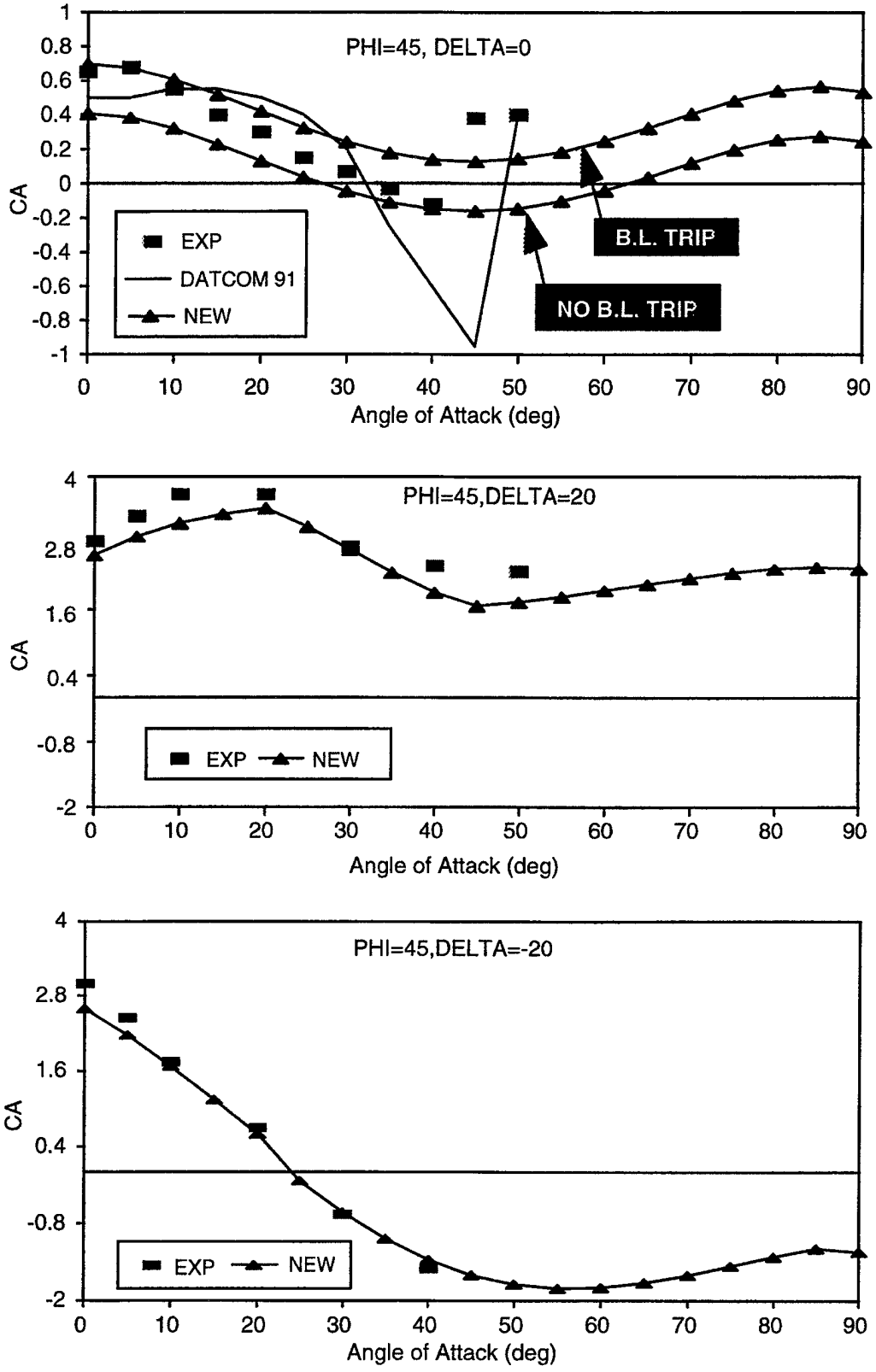

FIGURE 8C. COMPARISON OF THEORETICAL METHODS FOR AXIAL FORCE PREDICTION TO EXPERIMENT ON FIGURE 8A CONFIGURATION (Φ = 45 deg, M = 0.2, $R_N = 1.42 \times 10^{-6}$/ft)

It is also interesting to note that this experimental value of C_A is 0.64 versus that in Figure 8B of 0.45, although in principle the values should be approximately the same within measurement errors. This illustrates the point the authors of Reference 18 made with respect to the sting balance being defined for large normal forces resulting in inherently less accurate axial force measurements. Note that no AP95 results are shown on Figure 8C due to the fact the AP95 was only applicable at $\Phi = 0$ deg. Note that the $\Phi = 45$ deg, $\delta = \pm 20$ deg cases of Figure 8C show the new theory compares very well to experiment. It is particularly encouraging to see the theory predict the stall effect that occurs at $\delta = +20$ and $\alpha = 20$ to 45 deg. This is shown on Figure 8C with a fairly sharp drop in C_A above AOA 20 deg.

A wing-body-tail configuration where the wings are used for control was the next case considered in the validation process. This configuration is shown in Figure 9A with the experimental results given in Reference 20. This configuration has a length of about 18 calibers with a tangent ogive nose of 2.25 calibers in length. It has wings and tails of fairly high aspect ratios of 2.8 and 2.6 respectively. Data were taken at Mach numbers 1.5 to 4.63, for AOAs to 45 deg and control deflections of 0 and 10 deg at M of 1.5 and 2.0 and 0 to 20 deg at M of 2.35 to 4.63. The data were taken at a Reynolds number of 2.5×10^6/ft and boundary layer trips were also used. The model had a hollow chamber, and chamber axial force measurements were given separately in Reference 20. These results were added to the forebody axial force measurements to compare with the AP95 and new AOA axial force prediction method presented in this report.

Figures 9B through 9E show the comparisons of the new theory with the previous AP95 calculations and the data of Reference 20. Mach numbers 1.5, 2.35, 3.95 and 4.63 are shown in the comparisons. Figures 9B and 9C are the 0 deg control deflection results at $\Phi = 0$ and 45 deg, respectively. The theory gives the same results for these roll orientations at a given AOA and Mach number. As seen in the comparisons to data, there is a slight effect of roll on axial force, but not enough to account for in a semiempirical code for no control deflection. Figures 9D and 9E give the corresponding comparisons of theory to data[20] for $\Phi = 0$ and 45 deg roll respectively, but with control deflection. At $M_\infty = 1.5$, the control deflection is 10 deg, whereas at the other Mach numbers it is 20 deg. Here the theory does distinguish between roll of 0 and 45 deg, since only two fins are deflected at 0 deg roll whereas all four are deflected at 45 deg roll. Also note that no AP95 computations are shown on either Figure 9C or 9E due to the fact the AP95 is only applicable at $\Phi = 0$ deg. Note that in all the Figures 9B through 9E, the new method in general is equal to or superior to the AP95 and also gives very good agreement in comparison to data. The worst comparison is for M = 3.95, $\delta = 20$ deg, $\Phi = 0$ deg and AOA 40 deg. Even for this worst case comparison, the new theory differs from data by only 12 percent. The average accuracy errors of the new method to data in Figures 9B through 9E are well within the ±10 percent accuracy level claimed in the overall accuracy levels for normal and axial force coefficients.

The final configuration considered for validation is a wing-body-tail case where the tail surfaces are used for control. The configuration is identical to configuration 9A except the wing trailing edges are truncated with a height of 0.05 inches versus being sharp, as shown in Figure 9A. This means the drag of this configuration is slightly greater than the wing-controlled case due to the wing trailing edge base pressure drag. The wind tunnel data[21] were taken at a Reynolds number of 2.0×10^6/ft versus the wing controlled case of 2.5×10^6/ft. However, a boundary layer trip was used for both the tail and wing controlled models.

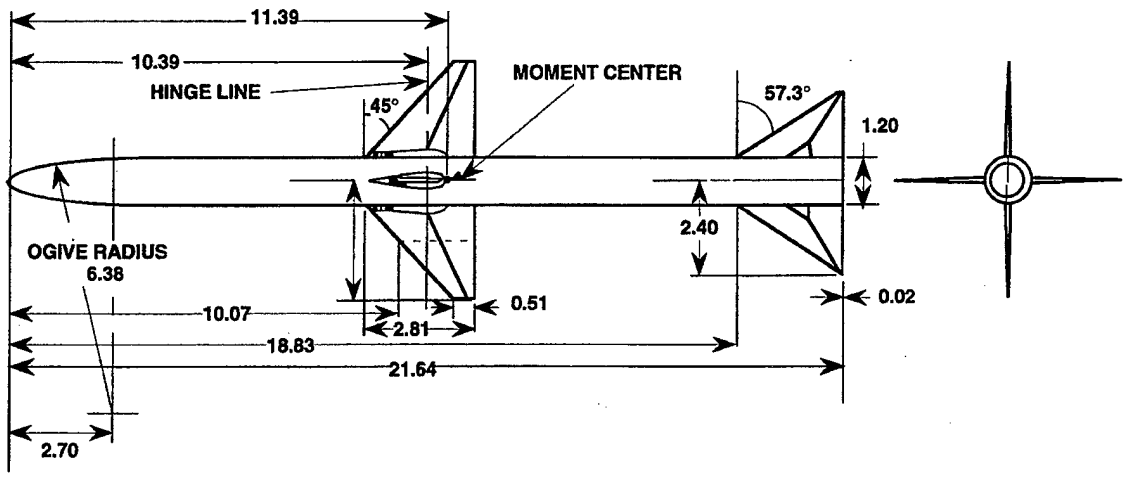

FIGURE 9A. AIR-TO-AIR MISSILE CONFIGURATION USED IN VALIDATION[20]

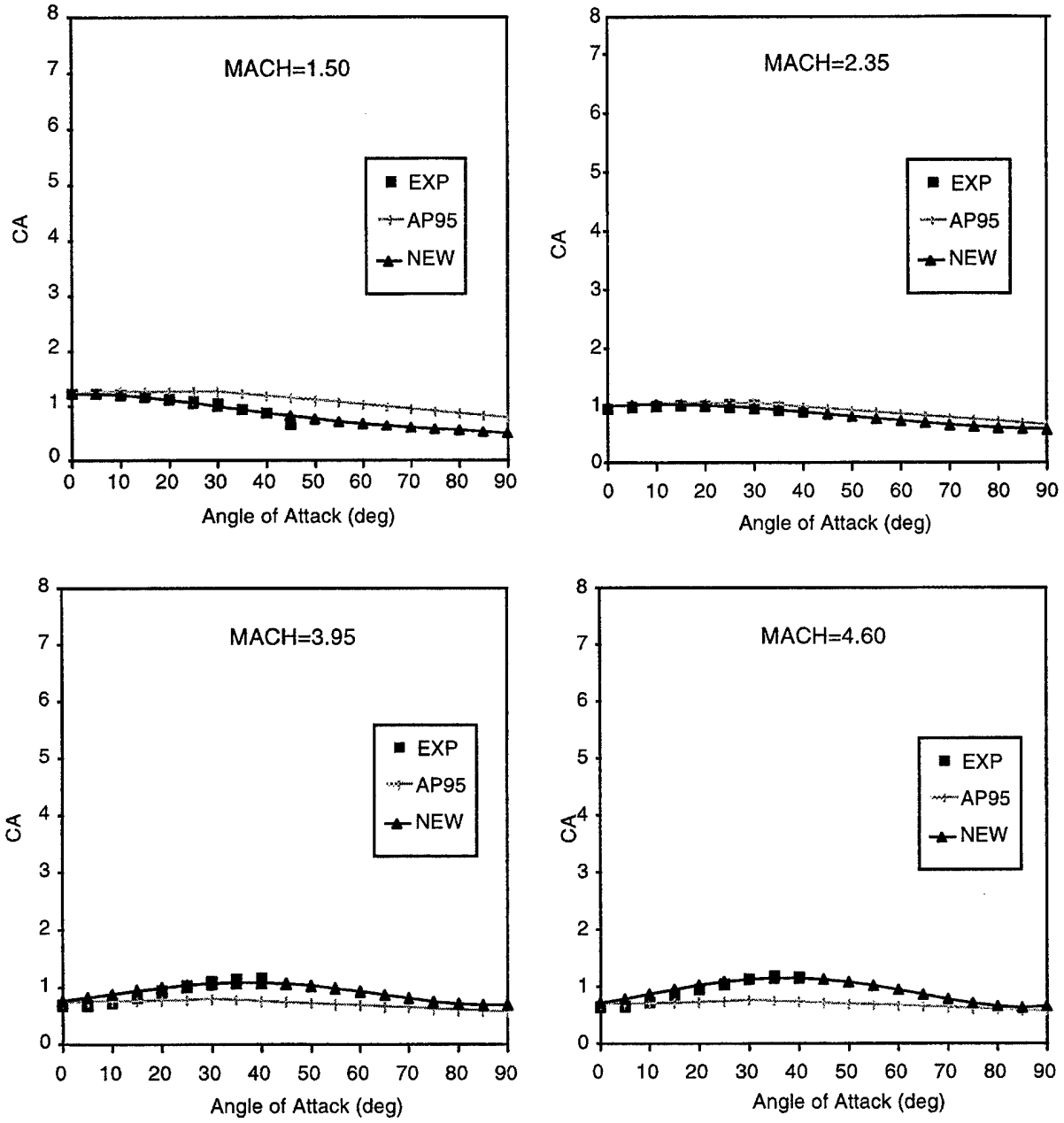

FIGURE 9B. COMPARISON OF THEORY AND EXPERIMENT FOR CONFIGURATION OF FIGURE 9A (Φ = 0 deg, δ = 0 deg)

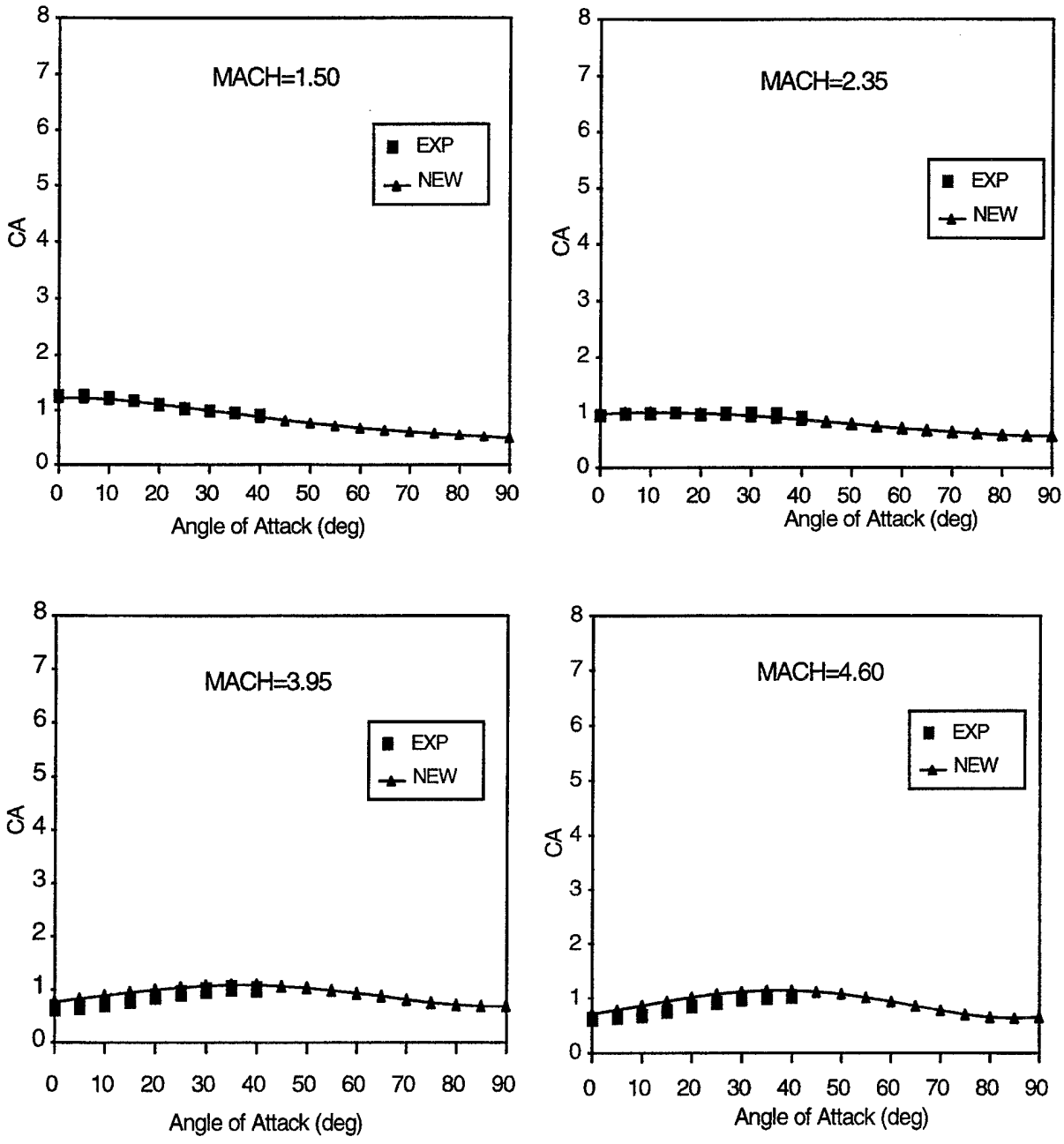

FIGURE 9C. COMPARISON OF THEORY AND EXPERIMENT FOR CONFIGURATION OF FIGURE 9A (Φ = 45 deg, δ = 0 deg)

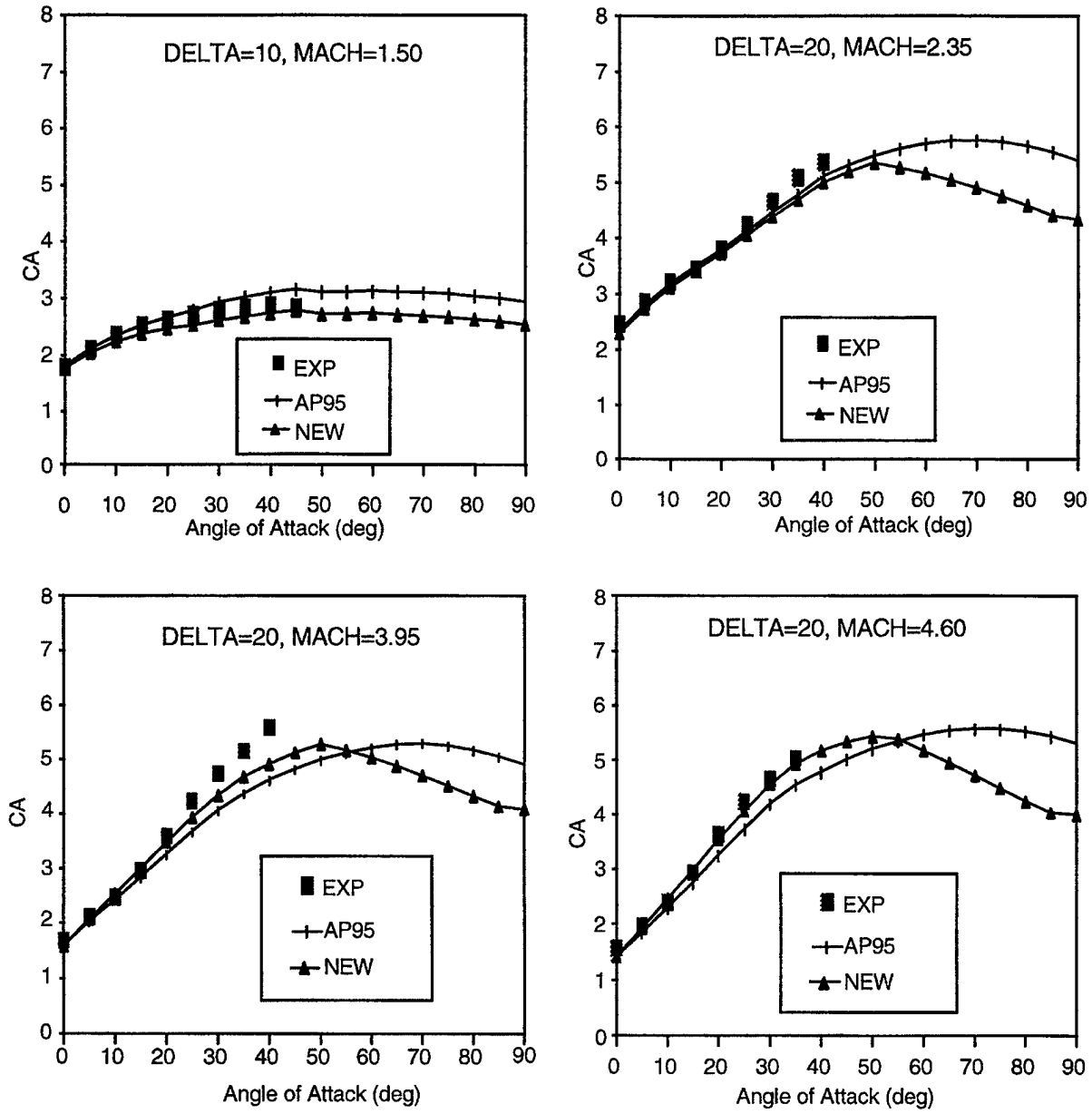

FIGURE 9D. COMPARISON OF THEORY AND EXPERIMENT FOR CONFIGURATION OF FIGURE 9A ($\Phi = 0$ deg)

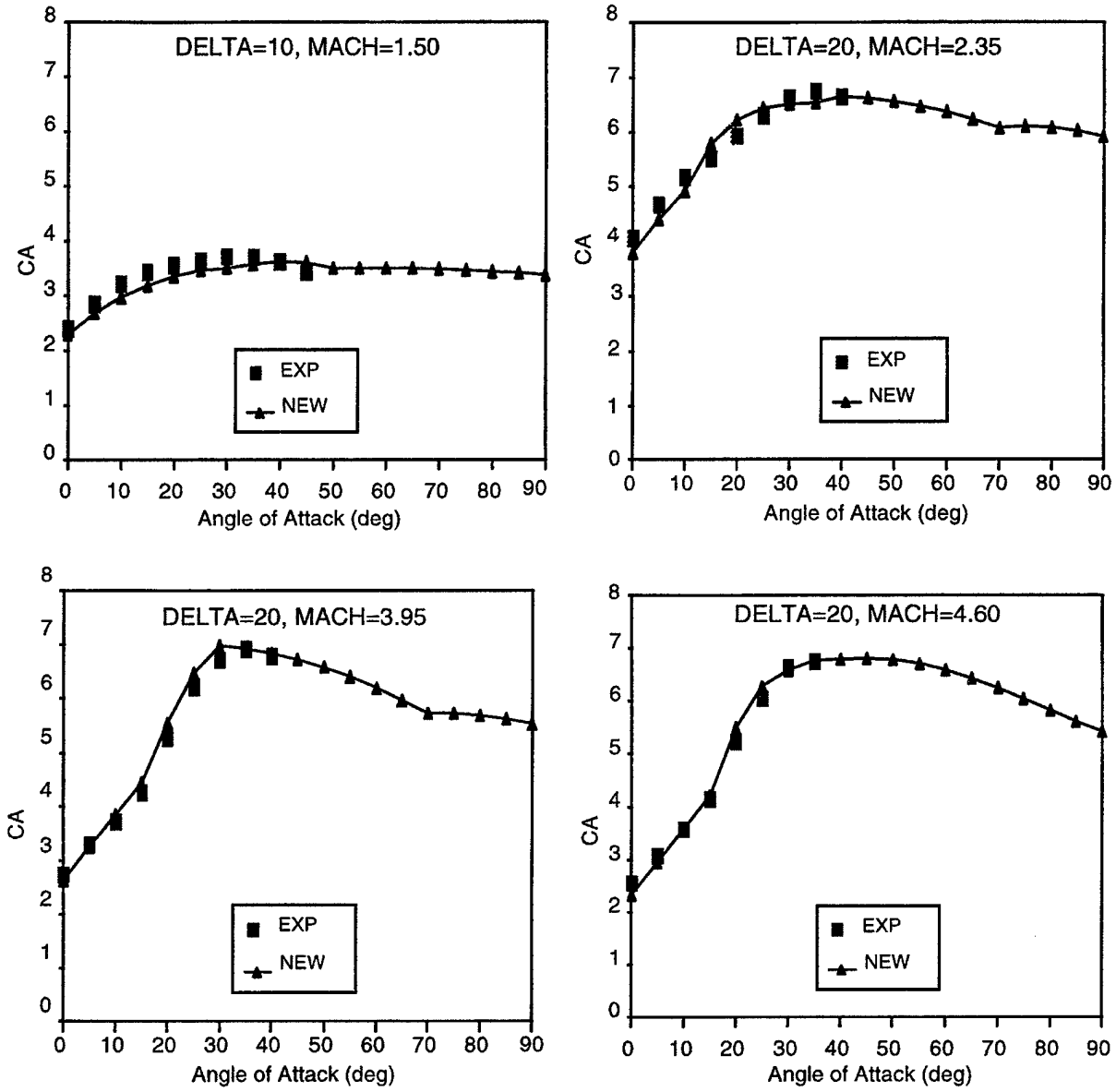

FIGURE 9E. COMPARISON OF THEORY AND EXPERIMENT FOR CONFIGURATION OF FIGURE 9A (Φ = 45 deg)

The comparisons of axial force coefficients to data[21] of the new method to the AP95 and experiment for no control deflection is quite similar to the results of Figures 9B and 9C and therefore will not be repeated here. The results for $\delta = -20$ deg at $\Phi = 0$ and $\Phi = 45$ deg are shown in Figures 10A and 10B respectively. Results are given in each figure for Mach numbers of 1. 5, 2.87, 3.85, and 4.6. The theory is shown up to AOA 90 deg although data are available only up to AOA of 35 deg. For Mach number of 1.5, both the AP95 and the new method appear to give acceptable results compared to data at both $\Phi = 0$ and $\Phi = 45$ deg. However, for the three higher Mach numbers, the new method is superior to the AP95 at both roll positions. The reason for this improved performance is due to the empirical model for AOA and control deflection of opposite signs as given in Figure 4.

4.0 SUMMARY AND RECOMMENDATIONS

An improved semiempirical method for axial force calculation on missile configurations has been developed. The method uses the theoretical methods currently used in the 1995 version of the NSWCDD Aeroprediction Code (AP95) for zero AOA axial force calculations and wind tunnel data bases to compute changes in axial force at AOA for body alone and wing-body configurations. Comparisons to data and existing theoretical approaches for computing the AOA contribution to axial force indicate the new method to be as good as or superior to existing techniques at all Mach numbers and AOAs. The improved method was also extended to configurations which have two sets of lifting surfaces and also to consider axial force due to control deflection. Comparisons of the extended method to the AP95 for wing-body-tail configurations showed improvements to the AP95 at higher AOA, higher Mach number and when the AOA and control deflection were of opposite sign.

In developing the improved semiempirical method several assumptions were necessary. These assumptions include:

a. The value of C_A at AOA 90 deg for configurations with 2 sets of lifting surfaces and for configurations with control deflections.

b. The value of C_A at high AOA outside the Mach number range for which data were available ($M > 4.6$).

c. How to break the contribution in C_A due to AOA into individual axial force components due to skin-friction, wave or pressure and base pressure.

As a result of these assumptions, it is recommended that Navier Stokes (N.S.) computations be conducted on a limited set of cases to try to sort out the axial force components. These computations should be conducted in conjunction with appropriate wind tunnel tests at high AOA for verification of the N.S. computations. It is then recommended that the current methodology be refined based on results from these wind tunnel data and N.S. computations.

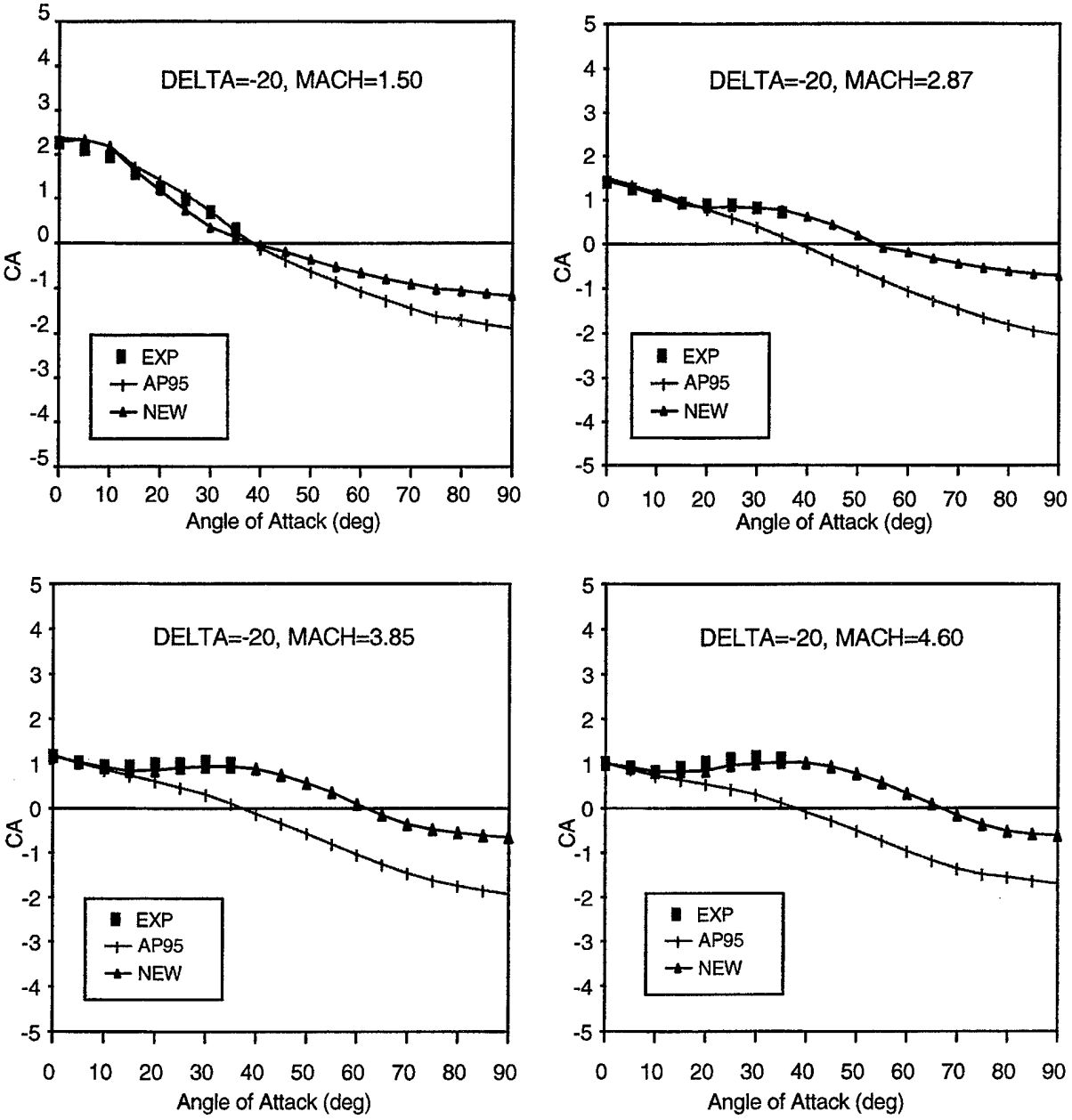

FIGURE 10A. COMPARISON OF AXIAL FORCE COEFFICIENTS OF A TAIL CONTROLLED WING-BODY-TAIL CONFIGURATION (Φ = 0 deg)

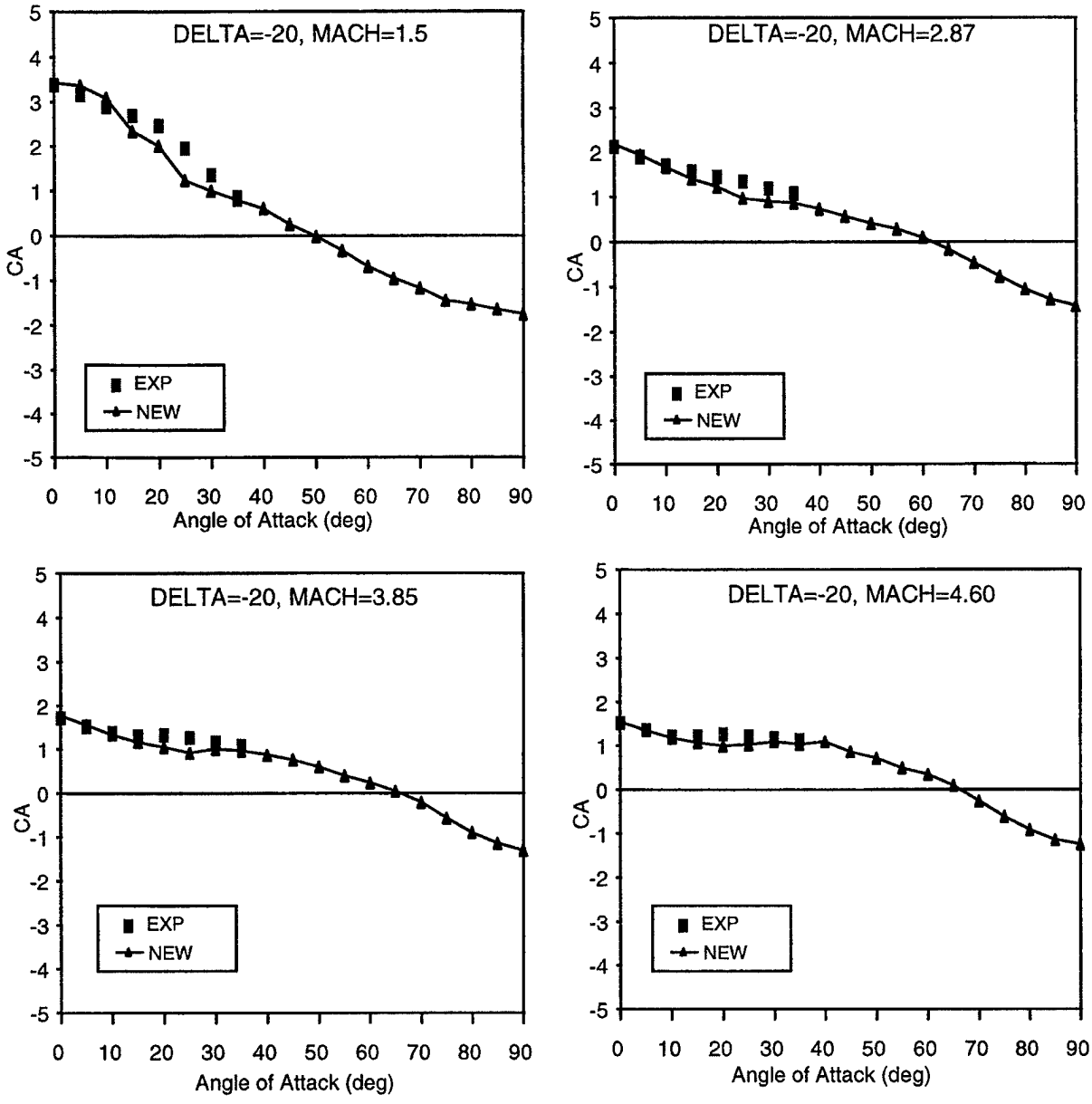

FIGURE 10B. COMPARISON OF AXIAL FORCE COEFFICIENTS OF A TAIL CONTROLLED WING-BODY-TAIL CONFIGURATION (Φ = 45 deg)

5.0 REFERENCES

1. Moore, F. G.; McInville, R. M.; and Hymer, T., *The 1995 Version of the NSWC Aeroprediction Code: Part I - Summary of New Theoretical Methodology*, NSWCDD/TR-94/379.

2. Jorgensen, L. H., *Prediction of Static Aerodynamic Characteristics for Slender Bodies Alone and with Lifting Surfaces to Very High Angles of Attack*, NASA TR R-474, Sep 1977.

3. Fidler, J. E. and Bateman, M. C., *Aerodynamic Methodology (Bodies with and Without Tails in Transonic Flow)*, report issued under U.S. Navy NAVAIR Contract N00019-73-C-0108, Commander, Naval Air Systems Command, Washington, DC, 1974.

4. Aiello, G. F. and Bateman, M. C., *Aerodynamic Stability Technology for Maneuverable Missiles*, AFFDL-TR-76-55, Vol. 1, AFFDL, Air Force Systems Command, Wright Patterson Air Force Base, OH, Dec 1976.

5. Ingram, C. W.; Ball, K.; Dinkeloo, C.; and Shida, D., *Preliminary Design Aerodynamic Prediction Methodology for Missiles with Nose Bluntness*, AFFDL-TR-78-117, AFFDL, Air Force Systems Command, Wright-Patterson Air Force Base, OH, Sep 1978.

6. Moore, F. G., *Body Alone Aerodynamics of Guided and Unguided Projectiles at Subsonic, Transonic and Supersonic Mach Numbers*, NWL TR 2796, NSWCDD, Dahlgren, VA, Nov 1972.

7. DeJarnette, F. R. and Jones, K. M., *Development of a Computer Program to Calculate Aerodynamic Characteristics of Bodies and Wing-Body Combinations*, NSWC/DL TR-3829, NSWCDD, Dahlgren, VA, Apr 1978.

8. Moore, F. G.; Armistead, M. A.; Rowles, S. H.; and DeJarnette, F. R., *Second-Order, Shock Expansion Theory Extended to Include Real Gas Effects*, NAVSWC TR-90-683, NSWCDD, Dahlgren, VA, Feb 1992.

9. Wu, J. M. and Aoyoma, K., *Transonic Flow-Field Calculation Around Ogive Cylinders by Nonlinear-Linear Stretching Method*, U.S. Army Missile Command TR-70-12, AMICOM, Huntsville, AL, Apr 1970.

10. Chaussee, D. S., *Improved Transonic Nose Drag Estimates for the NSWC Missile Aerodynamic Computer Program*, NSWC/DL TR-3830, NSWCDD, Dahlgren, VA, Apr 1978.

REFERENCES (Continued)

11. Devan, L., *Aerodynamics of Tactical Weapons to Mach Number 8 and Angle of Attack 180 °: Part I, Theory and Application*, NSWC TR 80-346, NSWCDD, Dahlgren, VA, Oct 1980.

12. Van Driest, E. R., "Turbulent Boundary Layers in Compressible Fluids," *Journal of Aeronautical Sciences*, Vol. 18, No. 3, 195 1, pp. 145-160, 216.

13. Moore, F. G.; Wilcox. F.; and Hymer, T., *Improved Empirical Model for Base Drag Prediction on Missile Configurations Based on New Wind Tunnel Data*, NSWCDD/TR-92/509, NSWCDD, Dahlgren, VA, Oct 1992.

14. NASA Langley Research Center Tri-Service Missile Data Base, Transmitted from NASA/LRC Jerry M. Allen to NSWCDD on 5 Nov 1991 (formal documentation in process).

15. Baker, W. B., *Static Aerodynamic Characteristics of a Series of Generalized Slender Bodies with and without Fins at Mach Numbers from 0.6 to 3.0 and Angles of Attack from 0 to 180 Deg*, AEDC TR-75-125, Vols. I and II, AEDC, Air Force Systems Command, Arnold Air Force Station, TN, May 1976.

16. Moore, F. and McInville, R. M., *Extension of the NSWCDD Aeroprediction Code to the Roll Position of 45 Degrees*, NSWCDD/TR-95/160, NSWCDD, Dahlgren, VA, Dec 1995.

17. Graves, E. and Fournier, R., *Stability and Control Characteristics at Mach Numbers of 0.2 to 4.63 of a Cruciform Air-to-Air Missile with Triangular Canard Controls and a Trapezoidal Wing*, NASA TM-X 3070, Nov 1974.

18. Smith, E. H.; Hebbar, S. K.; and Platzer, M., "Aerodynamic Characteristics of a Canard-Controlled Missile at High Angles of Attack," AIAA Paper No. 93-0763, Reno, NV, 11-14 Jan 1993.

19. Vukelich, S. R. and Jenkins, J. E., "Missile DATCOM: Aerodynamic Prediction on Conventional Missiles Using Component Build-Up Techniques," AIAA paper 84-0388, Reno, NV, 1984.

20. Monta, W. J., *Supersonic Aerodynamic Characteristics of a Sparrow III Type Missile Model with Wing Controls and Comparison with Existing Tail-Control Results*, NASA TP 1078, Nov 1977.

21. Monta, W. J., *Supersonic Aerodynamic Characteristics of an Air-to-Air Missile Configuration with Cruciform Wings and In-Line Tail Controls*, NASA TM S-2666, 1972.

6.0 SYMBOLS AND DEFINITIONS

AOA	Angle of Attack
AP72, AP95	1972 and 1995 versions, respectively, of the NSWCDD aeroprediction code
C_A	Axial force coefficient
C_{A_B}	That part of the axial force coefficient due to the base of the configuration
C_{A_f}	That part of the axial force coefficient due to skin friction
C_{A_O}	Axial force coefficient at AOA of zero degrees
C_{A_P}	That part of the axial force coefficient due to pressure on the body excluding the base region
C_{A_α}	Axial force coefficient component due to AOA
C_{A_δ}	Axial force coefficient component due to control deflection, δ
C_D	Drag coefficient
C_L	Lift coefficient
$f(M,\alpha)$, $f'(M,\alpha)$	Function and its derivative respectively, which are defined based on various data bases as a function of Mach number and AOA
L/D	Lift to drag ratio
M, M_∞	Mach number and freestream Mach numbers
MNT	Modified Newtonian Theory
α	Angle of Attack (degrees)
δ	Control deflection (degrees) with leading edge up as positive
Φ	Roll position with $\Phi = 0$ deg having fins in plus (+) roll orientation and $\Phi = 45$ deg having fins in cross (×) roll position

DISTRIBUTION

DOD ACTIVITIES (CONUS)

		Copies
ATTN	CODE 04 (BISSON)	1
	CODE 30	1
	CODE 44 (ZIMET)	1
	CODE 4425 (SIEGEL)	1
	CODE 332FD (LEKOUDIS)	1
	CODE 442 (WOOD)	1

CHIEF OF NAVAL RESEARCH
BALLSTON CENTRE TOWER ONE
800 NORTH QUINCY ST
ARLINGTON VA 22217-5660

ATTN	CODE 474T6OD (LOFTUS)	1
	CODE 4732HOD (SMITH)	1
	CODE 4732HOD (LAMBERT)	1
	CODE 473COOD (PORTER)	1
	CODE 47311OD (HOUSH)	1
	CODE 47311OD (GLEASON)	1
	CODE 47311OD (VAN DYKEN)	1
	CODE 4722EOD (JETER)	1
	TECHNICAL LIBRARY	1

COMMANDER
NAVAL AIR WARFARE CENTER
WEAPONS DIVISION
1 ADMINISTRATION CIRCLE
CHINA LAKE CA 93555-6001

ATTN	TECHNICAL LIBRARY	1
	G RUDACILLE PMS 38012 7	1

COMMANDER
NAVAL SEA SYSTEMS COMMAND
2531 JEFFERSON DAVIS HWY
ARLINGTON VA 22242-5160

ATTN	AIR 53012D (JOHNSON)	1
	RM 904 JP 2	
	TECHNICAL LIBRARY	1

COMMANDER
NAVAL AIR SYSTEMS COMMAND
HEADQUARTERS
1421 JEFFERSON DAVIS HWY
ARLINGTON VA 22243-5120

ATTN	C KLEIN	1
	TECHNICAL LIBRARY	1

COMMANDER
NAVAL AIR WARFARE CENTER
WEAPONS DIVISION
521 9TH ST
POINT MUGU CA 93042-5001

ATTN	T C TAI	1
	M J MALIA	1
	TECHNICAL LIBRARY	1

COMMANDER
NAVAL SHIP RESEARCH AND
DEVELOPMENT CENTER
WASHINGTON DC 20034

ATTN	R M HOWARD	1
	TECHNICAL LIBRARY	1

SUPERINTENDENT
NAVAL POSTGRADUATE SCHOOL
1 UNIVERSITY CIRCLE
MONTEREY CA 93943-5001

ATTN	S GREENHALGH	1
	C REITZ	1
	TECHNICAL LIBRARY	1

COMMANDING OFFICER
NAVAL AIR WARFARE CENTER
AIRCRAFT DIVISION WARMINSTER
BOX 5152
WARMINSTER PA 18974-0591

ATTN	HEAD WEAPONS DEPT	1
	HEAD SCIENCE DEPT	1

SUPERINTENDENT
UNITED STATES NAVAL ACADEMY
121 BLAKE RD
ANNAPOLIS MD 21402-5000

ATTN	TECHNICAL LIBRARY	1

OFFICER IN CHARGE
NAVAL INTELLIGENCE SUPPORT CENTER
4301 SUITLAND ROAD
ALEXANDRIA VA 22217

DISTRIBUTION (Continued)

	Copies
ATTN DIAG DT 4T (PAUL MURAD)	2
DIRECTOR	
DEFENSE INTELLIGENCE AGENCY	
WASHINGTON DC 20301	
ATTN BRENT WAGGONER	1
CODE 4072 BLDG 2540	
NAVAL WEAPONS SUPPORT CENTER	
CRANE IN 47522-5000	
ATTN CODE 5252P (KRAUSE)	1
TECHNICAL LIBRARY	1
COMMANDER	
INDIAN HEAD DIVISION	
NAVAL SURFACE WARFARE CENTER	
101 STRAUSS AVE	
INDIAN HEAD MD 20640-5035	
ATTN TECHNICAL LIBRARY	1
COMMANDING GENERAL	
MARINE CORPS COMBAT	
DEVELOPMENT COMMAND	
2048 SOUTH ST	
QUANTICO VA 22134-5129	
ATTN E SEARS	1
L E LIJEWSKI	1
C COTTRELL	1
TECHNICAL LIBRARY	1
AFATL (ADLRA) (DLGC)	1
EGLIN AFB FL 32542-5000	
ATTN TECHNICAL LIBRARY	1
USAF ACADEMY	
COLORADO SPRINGS CO 80912	
ATTN TECHNICAL LIBRARY	1
ADVANCED RESEARCH PROJECTS AGENCY	
DEPARTMENT OF DEFENSE	
WASHINGTON DC 20305	

	Copies
ATTN B BLAKE (BLD 146)	1
D SHEREDA (BLD 450)	1
J JENKINS (BLD 146)	1
R SAMUELS (BLD 856)	1
TECHNICAL LIBRARY	1
COMMANDING OFFICER	
AFSC	
2210 8TH STREET	
WRIGHT PATTERSON AFB OH 45433	
ATTN EDWARD JENKINS	1
NAIC TANW	
HQ NAIC TANW	
4115 HEBBLE CREEK ROAD SUITE 28	
WPAFB OH 45433-5623	
ATTN J USSELTON	1
W B BAKER JR	1
TECHNICAL LIBRARY	1
ARNOLD ENGINEERING DEVELOPMENT CENTER USAF	
TULLAHOMA TN 37389	
ATTN H HUDGINS	1
G FRIEDMAN	1
TECHNICAL LIBRARY	1
COMMANDING GENERAL	
ARRADCOM PICATINNY ARSENAL	
DOVER NJ 07801	
ATTN C H MURPHY	1
R PUHALLA JR	1
W STUREK	1
C NIETUBICZ	1
A MIKHAIL	1
P PLOSTINS	1
TECHNICAL LIBRARY	1
COMMANDING GENERAL	
BALLISTIC RESEARCH LABORATORY	
ABERDEEN PROVING GROUND	
ABERDEEN MD 21005-5066	

DISTRIBUTION (Continued)

	Copies
ATTN CODE TNC (BLACKLEDGE)	1
RICH MATLOCK	1
DIRECTOR	
INTERCEPTOR TECHNOLOGY	
BALLISTIC MISSILE DEFENSE OFFICE	
THE PENTAGON	
WASHINGTON DC 20350	
ATTN SFAE SD ASP	1
SFAE SD HED	1
DEPUTY COMMANDER	
US ARMY STRATEGIC DEFENSE COMMAND	
P O BOX 1500	
HUNTSVILLE AL 35807-3801	
ATTN D WASHINGTON	1
W WALKER	1
R KRETZSCHMAR	1
D FERGUSON JR	1
COMMAND GENERAL	
US ARMY MISSILE COMMAND	
AMSMI RD SS AT	
REDSTONE ARSENAL AL 35898-5252	
DEFENSE TECHNICAL INFORMATION CENTER	
8725 JOHN J KINGMAN ROAD	
SUITE 0944	
FORT BELVOIR VA 22060-6218	2
DIRECTOR	
DEFENSE PRINTING SERVICE	
BLDG 176 WASHINGTON NAVY YARD	
901 M ST E	
WASHINGTON DC 20374-5087	1
ATTN CODE A76	
TECHNICAL LIBRARY	1
COMMANDING OFFICER	
COASTAL SYSTEMS STATION	
DAHLGREN DIVISION	
NAVAL SURFACE WARFARE CENTER	
6703 W HIGHWAY 98	
PANAMA CITY FL 32407-7001	

	Copies
ATTN DR P WEINACHT	1
AERODYNAMICS BRANCH	
PROPULSION AND FLIGHT DIV WTD	
AMSRL WT PB	
US ARMY RESEARCH LAB ABERDEEN	
PROVING GROUND MD 21005-5066	
ATTN GREGG ABATE	1
US AIR FORCE	
WRIGHT LABORATORY	
WL MNAA	
101 W EGLIN BLVD STE 219	
EGLIN AFB FL 32542	
ATTN JOHN GRAU	1
US ARMY ARDEC	
COMMANDER US ARMY ARDEC	
AMSTA AR AET A BLDG 3342	
PICATINNY ARSENAL NJ 07806-5000	
ATTN FRANK MACDONALD	1
NAWC CHINA LAKE	
COMMANDER	
CODE 473 20D	
NAVAIRWARCENNSDNDIV	
CHINA LAKE CA 93555	
ATTN MARK LAMBERT	1
NAWC	
CODE 4732HOD	
CHINA LAKE CA 93555	
ATTN MICHAEL MUSACHIO	1
DIRECTOR	
OFFICE OF NAVAL INTELLIGENCE	
4251 SUITLAND ROAD (ONI 2321)	
WASHINGTON DC 20395	
ATTN DR ALAN NICHOLSON MSC 5B	1
DEFENSE INTELLIGENCE AGENCY	
MISSILE AND SPACE INTELLIGENCE CTR	
REDSTONE ARSENAL AL 35898-5500	
ATTN EDWARD HERBERT	1
US ARMY MISSILE COMMAND	
AMSMI RD MG GA	
BLDG 5400 ROOM 250	
REDSTONE ARSENAL AL 35898	

DISTRIBUTION (Continued)

	Copies
ATTN PAUL KOLODZIEJ NASA AMES RESEARCH CENTER MS 234 1 MOFFETT FIELD CA 94035	1
ATTN LCDR T HARTLINE USNR R NR ONI 2109 NAVAL RESERVE UNIT 112 CRESTVIEW CIRCLE MADISON AL 35758	1
ATTN CODE 4732HOD DAVID HALL PROPULSION PERFORMANCE OFFICE NAVAL AIR WARFARE CTR WEAPONS DIV 1 ADMINISTRATIVE CIR CHINA LAKE CA 93555-6001	1
NON-DOD ACTIVITIES (CONUS)	
ATTN NEIL WALKER NICHOLS RESEARCH CORPORATION MS 912 P O BOX 400002 4040 S MEMORIAL PKWY HUNTSVILLE AL 35815-1502	1
THE CNA CORPORATION P O BOX 16268 ALEXANDRIA VA 22302-0268	1
ATTN GIFT AND EXCHANGE DIVISION LIBRARY OF CONGRESS WASHINGTON DC 20540	4
GIDEP OPERATIONS OFFICE CORONA CA 91720	1
ATTN TECHNICAL LIBRARY NASA AMES RESEARCH CENTER MOFFETT CA 94035-1099	1
ATTN C SCOTT D CURRY NASA JOHNSON SPACE CENTER HOUSTON TX 77058	1 1
ATTN TECHNICAL LIBRARY NASA WASHINGTON DC 20546	1
ATTN W C SAWYER B HENDERSON D MILLER J ALLEN F WILCOX TECHNICAL LIBRARY NASA LANGLEY RESEARCH CENTER HAMPTON VA 23365	1 1 1 1 1 2
ATTN D G MILLER (L 219) TECHNICAL LIBRARY LAWRENCE LIVERMORE NATIONAL LABORATORY EARTH SCIENCES DIVISION UNIVERSITY OF CALIFORNIA P O BOX 808 LIVERMORE CA 94551	1 1
ATTN W RUTLEDGE (1635) R LAFARGE R EISLER TECHNICAL LIBRARY SANDIA NATIONAL LABORATORY P O BOX 5800 ALBUQUERQUE NM 87185-5800	1 1 1 1
ATTN WALT GUTIERREZ SANDIA NATIONAL LABORATORIES MAIL STOP 0825 P O BOX 5800 ALBUQUERQUE NM 87185-0825	1
ATTN ASSISTANT DEFENSE COOPERATION ATTACHE EMBASSY OF SPAIN WASHINGTON DC 20016	1
ATTN CDR R TEMPEST BRITISH NAVY STAFF WASHINGTON DC 20008	1
ATTN ASO LO IS ISRAEL AIR FORCE LIAISON OFFICER 700 ROBBINS AVE PHILADELPHIA PA 19111	1

DISTRIBUTION (Continued)

	Copies
ATTN GERMAN MILITARY REP US OA GMR TRAFFIC AND TRANSPORTATION DIVISION 10 SERVICES ROAD DULLES INTERNATIONAL AP WASHINGTON DC 20041	1
ATTN F D DEJARNETTE NORTH CAROLINA STATE UNIVERSITY DEPT OF MECHANICAL AND AEROSPACE ENGINEERING BOX 7921 RALEIGH NC 27695	1
ATTN PROF J A SCHETZ VIRGINIA POLYTECHNIC AND STATE UNIVERSITY DEPT OF AEROSPACE ENGINEERING BLACKSBURG VA 24060	1
ATTN J M WU C BALASUBRAMAYAN TECHNICAL LIBRARY THE UNIVERSITY OF TENNESSEE SPACE INSTITUTE TULLAHOMA TN 37388	1 1 1
ATTN R NELSON TECHNICAL LIBRARY UNIVERSITY OF NOTRE DAME DEPT OF AEROSPACE AND MECHANICAL ENGINEERING BOX 537 NOTRE DAME IN 46556	1 1
ATTN PROF F NELSON DEPT OF MECH AND AERO ENG UNIVERSITY OF MISSOURI ROLLA ROLLA MO 65401	1
ATTN DR DONALD SPRING AEROSPACE ENGINEERING DEPT AUBURN UNIVERSITY AL 36849-5338	1
ATTN ROBERT ENGLAR GEORGIA TECH RESEARCH INSTITUTE AEROSPACE SCIENCE AND TECHNOLOGY LAB ATLANTA GA 30332	1
ATTN E LUCERO L TISSERAND D FROSTBUTTER L PERINI TECHNICAL LIBRARY APPLIED PHYSICS LABORATORY JOHNS HOPKINS UNIVERSITY JOHNS HOPKINS ROAD LAUREL MD 20723-6099	1 1 1 1 1
ATTN B BROOKS R STANCIL R ELKINS LORAL VOUGHT SYSTEMS P O BOX 650003 M S EM 55 DALLAS TX 75265-0003	1 1 1
ATTN TECHNICAL LIBRARY MARTIN MARIETTA AEROSPACE P O BOX 5837 ORLANDO FL 32805	1
ATTN R CAVAGE ADVANCED SYSTEMS DESIGN DEPT 113 407 (GB14) ROCKWELL NORTH AMERICAN AIRCRAFT OPERATIONS P O BOX 3644 SEAL BEACH CA 90740-7644	1
ATTN TECHNICAL LIBRARY HUGHES MISSILE SYSTEMS COMPANY P O BOX 11337 BLDG 802 MS A1 OLD NOGALES HWY TUCSON AZ 83734-1337	1

DISTRIBUTION (Continued)

	Copies
ATTN M DILLENIUS	1
NIELSEN ENGINEERING AND RESEARCH INC	
526 CLYDE AVE	
MOUNTAIN VIEW CA 95043	
ATTN J XERIKOS	1
N CAMPBELL	1
TECHNICAL LIBRARY	1
MCDONNEL DOUGLAS ASTRONAUTICS CO (WEST)	
5301 BOLSA AVE	
HUNTINGTON BEACH CA 92647	
ATTN J WILLIAMS	1
S VUKELICH	1
J FIVEL	1
R GERBSCH (CODE 1111041)	1
TECHNICAL LIBRARY	1
MCDONNELL DOUGLAS ASTRONAUTICS CO (EAST)	
BOX 516	
ST LOUIS MO 63166-0516	
ATTN TECHNICAL LIBRARY	1
UNITED TECHNOLOGIES	
NORDEN SYSTEMS	
NORWALK CT 06856	
ATTN T LUNDY	1
D ANDREWS	1
TECHNICAL LIBRARY	1
LOCKHEED MISSILES AND SPACE CO INC	
P O BOX 1103	
HUNTSVILLE AL 35807	
ATTN W CHRISTENSON	1
D WARNER	1
ALLIANT TECHSYSTEMS INC	
600 SECOND ST NE	
HOPKINS MN 55343	
ATTN TECHNICAL LIBRARY	1
B SALEMI	1
J BOUDREAU	1
RAYTHEON COMPANY	
MISSILE SYSTEMS DIVISION	
P O BOX 1201	
TEWKSBURY MA 01876-0901	
ATTN LLOYD PRATT	1
AEROJET TACTICAL SYSTEMS CO	
P O BOX 13400	
SACRAMENTO CA 95813	
ATTN JOSEPH ANDRZEJEWSKI	1
MEVATEC CORP	
1525 PERIMETER PARKWAY	
SUITE 500	
HUNTSVILLE AL 35806	
ATTN DR G S SCHMIDT	1
LORAL DEFENSE SYSTEMS	
1210 MASSILLON ROAD	
AKRON OH 44315-0001	
ATTN W NORDGREN 721	1
GOULD INC OSD	
18901 EUCLID AVE	
CLEVELAND OH 44117	
ATTN TECH LIBRARY	1
AEROJET ELECTRONIC SYSTEMS	
P O BOX 296 III	
AZUSA CA 91702	
ATTN P REDING	1
G CHRUSCIEL	1
TECHNICAL LIBRARY	1
LOCKHEED MISSILES AND SPACE CO INC	
P O BOX 3504	
SUNNYVALE CA 94088	
ATTN K C LEE	1
AEROTHERM CORP	
580 CLYDE AVE	
MOUNTAIN VIEW CA 94043	

DISTRIBUTION (Continued)

	Copies
ATTN TECH LIBRARY FMC NAVAL SYSTEMS DIV 4800 E RIVER ROAD MINNEAPOLIS MN 55421-1402	1
ATTN DORIA GLADSTONE BATTELLE MEMORIAL INSTITUTE COLUMBUS DIVISION 505 KING AVE COLUMBUS OH 43201-2693	1
ATTN JAMES SORENSON VINCENT ALLEN ORBITAL SCIENCES 3380 SOUTH PRICE ROAD CHANDLER AZ 85248	1 1
ATTN J FORKOIS KAMAN SCIENCES CORP 1500 GARDEN OF THE GODS ROAD P O BOX 7463 COLORADO SPRINGS CO 80933	1
ATTN FRED KAUTZ MIT LINCOLN LABORATORY LEXINGTON MA 02173-0073	1
ATTN D J GIESE MAIL STOP 4C 61 BOEING DEFENSE AND SPACE GROUP P O BOX 3999 SEATTLE WA 98124-2499	1
ATTN W J CLARK DYNA EAST CORPORATION 3132 MARKET ST PHILADELPHIA PA 19104	1
ATTN BRIAN WALKUP HERCULES AEROSPACE PRODUCT CO ALLEGHANY BALLISTIC LAB ROCKET CENTER WV 26726	1
ATTN B D PRATS MARTIN MARIETTA ASTROSPACE AEROTHERMOPHYSICS 230 E GODDARD BLVD KING OF PRUSSIA PA 19406	1
ATTN DR T LIN TRW ELECTRONICS AND DEFENSE SECTOR BLDG 527/RM 706 P O BOX 1310 SAN BERNADINO CA 92402	1
ATTN G VINCENT SPARTA INC 4901 CORPORATE DR HUNTSVILLE AL 35805	1
ATTN D P FORSMO TECHNICAL LIBRARY RAYTHEON COMPANY MISSILE SYSTEMS DIVISION HARTWELL RD BEDFORD MA 01730-2498	1 1
ATTN M S MILLER BRIAN EST DYNETICS INC P O DRAWER B HUNTSVILLE AL 35814-5050	1 1
ATTN H A MCELROY GENERAL DEFENSE CORP P O BOX 127 RED LION PA 17356	1
ATTN R SEPLAK BRUNSWICK CORP DEFENSE DIVISION 3333 HARBOR BLVD COSTA MESA CA 92628-2009	1
ATTN J W MCDONALD GENERAL RESEARCH CORP ADVANCED TECHNOLOGY INC 5383 HOLLISTER AVE P O BOX 6770 SANTA BARBARA CA 93160-6770	1
ATTN CAROL BUTLER OTI INTERNATIONAL 60 2ND ST SUITE 301 P O BOX 37 SHALIMAR FL 32579	1

DISTRIBUTION (Continued)

	Copies
ATTN ENGINEERING LIBRARY ARMAMENT SYSTEMS DEPT GENERAL ELECTRIC CO BURLINGTON VT 05401	1
ATTN TECHNICAL LIBRARY OAYNE AERONAUTICAL 2701 HARBOR DRIVE SAN DIEGO CA 92138	1
ATTN WILLIAM FACINELLI ALLIED SIGNAL P O BOX 22200 MS 1207 3B TEMPE AZ 85285	1
ATTN DR T P SHIVANANDA TRW BMD P O BOX 1310 SAN BERNADINO CA 92402-1313	1
ATTN T R PEPITONE AEROSPACE TECHNOLOGY INC P O BOX 1809 DAHLGREN VA 22448	1
ATTN ERIC MOORE MAIL STOP MER 24 1281 LOCKHEED SANDERS P O BOX 868 NASHUA NH 03061	1
ATTN DR BRIAN LANDRUM RI BLDG E33 PROPULSION RESEARCH CENTER UNIVERSITY OF ALABAMA HUNTSVILLE AL 35899	1
ATTN BRUCE NORTON MAIL STOP BL 1 RAYTHEON 100 VANCE TANK RD BRISTOL TN 37620	1
ATTN JIM ROBERTSON RESEARCH SOUTH INC 555 SPARKMAN DRIVE SUITE 818 HUNTSVILLE AL 35816-3423	1
ATTN BOB WHYTE ARROW TECH ASSOCIATES INC 1233 SHELBURNE ROAD D8 SO BURLINGTON VT 05403	1
ATTN JUAN AMENABAR SAIC 4001 NORTH FAIRFAX DRIVE STE 800 ARLINGTON VA 22209	1
ATTN TECHNICAL LIBRARY TELEDYNE RYAN AERONAUTICAL 2701 HARBOR DRIVE SAN DIEGO CA 92138	1
ATTN DR KIRIT PATEL SVERDRUP TECHNOLOGY INC TEAS GROUP BLDG 260 P O BOX 1935 EGLIN AFB FL 32542	1
ATTN FRANK LANGHAM MICRO CRAFT TECHNOLOGY 740 4TH ST MS 6001 ARNOLD AFB TN 37389	1
ATTN LAURA AYERS DELTA RESEARCH INC 315 WYNN DRIVE SUITE 1 HUNTSVILLE AL 35805	1
ATTN BRIAN BENNETT MCDONNELL DOUGLAS MC 064 2905 P O BOX 516 ST LOUIS MO 63166-0516	1

DISTRIBUTION (Continued)

	Copies
ATTN THOMAS FARISS LOCKHEED SANDERS P O BOX 868 MER24 1206 NASHUA NH 03061-0868	1
ATTN COREY FROST LOCKHEED MISSILES & SPACE CO INC P O BOX 070017 6767 OLD MADISON PIKE SUITE 220 HUNTSVILLE AL 35807	1
ATTN JEFFREY HUTH KAMAN SCIENCES CORPORATION 2560 HUNTINGTON AVE ALEXANDRIA VA 22303	1
ATTN WILLIAM JOLLY KAMAN SCIENCES 600 BLVD SOUTH SUITE 208 HUNTSVILLE AL 35802	1
ATTN STEPHEN MALLETTE KBM ENTERPRISES 15980 CHANEY THOMPSON RD HUNTSVILLE AL 35803	1
ATTN DONALD MOORE NICHOLS RESEARCH CORPORATION 4040 SOUTH MEMORIAL PARKWAY P O BOX 400002 MS 920C HUNTSVILLE AL 35815-1502	1
ATTN JAY NARAIN LOCKHEED MISSILES & SPACE CO P O BOX 3504 DEPT 81 10 BLDG 157 5E FAE 1 SUNNYVALE CA 94088-3504	1
ATTN DAVID RESSLER TRW BALLISTIC MISSILES DIV MS 953 2420 P O BOX 1310 SAN BERNARDINO CA 92402	1
ATTN MARK SWENSON ALLIANT TECHSYSTEMS MN11 262B 600 SECOND STREET NE HOPKINS MN 55343	1
ATTN JOHN SUN NORTHROP GRUMMAN CORPORATION 750 LYNNMERE DRIVE THOUSAND OAKS CA 91360	1
ATTN HARRY AULTMAN COLEMAN RESEARCH CORP 6820 MOQUIN DRIVE HUNTSVILLE AL 35806	1
ATTN SCOTT ALLEN ALLEN AERO RESEARCH 431 E SUNNY HILLS RD FULLERTON CA 92635	1
ATTN DARRYL HALL SAIC 997 OLD EAGLE SCHOOL RD SUITE 215 WAYNE PA 19087-1803	1
ATTN PETER ALEXANDER MCDONNELL DOUGLAS AEROSPACE 689 DISCOVERY DRIVE MS 11A1 HUNTSVILLE AL 35806	1
ATTN SAMUEL HICKS III TEXAS INSTRUMENTS 6600 CHASE OAKS BLVD MS 8490 PLANO TX 75086	1
ATTN BARRY LINDBLOM ALLIANT DEFENSE ELECTRONICS SYSTEMS INC P O BOX 4648 CLEARWATER FL 34618	1

DISTRIBUTION (Continued)

	Copies
ATTN DR SHIN CHEN THE AEROSPACE CORP M4 967 P O BOX 92957 LOS ANGELES CA 90009	1
ATTN ROBERT ACEBAL SAIC 1225 JOHNSON FERRY RD SUITE 100 MARIETTA GA 30068	1
ATTN EUGENE HART SYSTEM PLANNING CORP 1000 WILSON BLVD ARLINGTON VA 22209	1
ATTN ELAINE POLHEMUS ROCKWELL AUTONETICS & MISSILE SYSTEMS DIVISION D611 DL23 1800 SATELLITE BLVD DULUTH GA 30136	1
ATTN MICHAEL GLENN TASC 1992 LEWIS TURNER BLVD FT WALTON BEACH FL 32547	1
ATTN ROBERT ROGER ADAPTIVE RESEARCH 4960 CORPORATE DRIVE SUITE 100 A HUNTSVILLE AL 35805-6229	1
ATTN STEVEN MARTIN SYSTEMS ENGINEERING GROUP INC 9841 BROKEN LAND PARKWAY SUITE 214 COLUMBIA MD 21046-1120	1
ATTN C W GIBKE LOCKHEED MARTIN VOUGHT SYSTEMS MS SP 72 P O BOX 650003 DALLAS TX 75265-0003	1
ATTN CHRIS HUGHES EDO GOVERNMENT SYSTEMS DIV 14 04 111TH ST COLLEGE POINT NY 11356	1
ATTN DANIEL LESIEUTRE NIELSEN ENGINEERING & RES INC 526 CLYDE AVENUE MOUNTAIN VIEW CA 94043-2212	1
ATTN CARL HILL FRANCIS PRIOLO STANDARD MISSILE COMPANY LLC 1505 FARM CREDIT DRIVE SUITE 600 MCLEAN VA 22102	1 1
ATTN THOMAS LOPEZ COLEMAN RESEARCH CORP 990 EXPLORER BLVD HUNTSVILLE AL 35806	1
ATTN JENNIE FOX LOCKHEED MARTIN VOUGHT SYSTEMS P O BOX 650003 MS EM 55 DALLAS TX 75265-0003	1
ATTN JOHN BURKHALTER AUBURN UNIVERSITY 211 AEROSPACE ENGR BLDG AUBURN UNIVERSITY AL 36849	1
ATTN DR MAX PLATZER NAVAL POSTGRADUATE SCHOOL DEPT OF AERONAUTICS & ASTRONAUTICS CODE AA PL MONTEREY CA 93943	1
ATTN MIKE DANGELO MIT LINCOLN LABORATORY 1745 JEFFERSON DAVIS HWY 1100 ARLINGTON VA 22202	1

DISTRIBUTION (Continued)

	Copies
ATTN LT BAHMAN ZOHURI NAVAL ACADEMY WEAPONS SYSTEMS ENGRG DEPT 121 BLAKE ROAD ANNAPOLIS MD 21402-5000	1
ATTN RICHARD HAMMER JOHNS HOPKINS APPLIED PHYSICS LAB JOHNS HOPKINS ROAD LAUREL MD 20723-6099	1
NON-DOD ACTIVITIES (EX-CONUS)	
ATTN LOUIS CHAN INSTITUTE FOR AEROSPACE RESEARCH NATIONAL RESEARCH COUNSIL MONTREAL RD OTTAWA ONTARIO CANADA K1A0R6	1
ATTN H B ASLUND SAAB MILITARY AIRCRAFT 581 88 LINKOEPING SWEDEN	1
ATTN R BARDWELL DEFENSE SYSTEMS LTD THE GROVE, WARREN LANE STANMORE, MIDDLESEX UNITED KINGDOM	1
ATTN A BOOTH BRITISH AEROSPACE DEFENCE LTD MILITARY AIRCRAFT DIVISION WARTON AERODROME WARTON PRESTON LANCASHIRE PR4 1AX UNITED KINGDOM	1
ATTN R CAYZAC GIAT INDUSTRIES 7 ROUTE DE GUERCY 18023 BOURGES CEDEX FRANCE	1
ATTN MAJ F DE COCK ECOLE ROYALE MILITAIRE 30 AV DE LA RENAISSANCE 1040 BRUXELLES BELGIUM	1
ATTN J EKEROOT BOFORS MISSILES 691 80 KARLSKOGA SWEDEN	1
ATTN CH FRANSSON NATIONAL DEFENCE RESEARCH ESTABLISHMENT DEPT OF WEAPON SYSTEMS EFFECTS AND PROTECTION KARLAVAGEN 106B 172 90 SUNDBYBERG SWEDEN	1
ATTN M HARPER BOURNE DEFENCE RESEARCH AGENCY Q134 BUILDING RAE FARNBOROUGH HAMPSHIRE QU14 6TD UNITED KINGDOM	1
ATTN A H HASSELROT FFA P O BOX 11021 161 11 BROMMA SWEDEN	1
ATTN B JONSSON DEFENCE MATERIAL ADMINISTRATION MISSILE TECHNOLOGY DIVISION 115 88 STOCKHOLM SWEDEN	1
ATTN P LEZEAUD DASSAULT AVIATION 78 QUAI MARCEL DASSAULT 92214 SAINT-CLOUD FRANCE	1

DISTRIBUTION (Continued)

	Copies
ATTN J LINDHOUT N L R ANTHONY FOKKERWEG 2 1059 CM AMSTERDAM THE NETHERLANDS	1
ATTN A MICKELLIDES GEC MARCONI DEFENCE SYSTEMS LTD THE GROVE WARREN LANE STANMORE MIDDLESEX UNITED KINGDOM	1
ATTN K MOELLER BODENSEEWERK GERAETETECHNIK GMBH POSTFACH 10 11 55 88641 UBERLINGEN GERMANY	1
ATTN G MOSS ROYAL MILITARY COLLEGE AEROMECHANICAL SYSTEMS GROUP SHRIVENHAM SWINDON WILTS SN6 8LA UNITED KINGDOM	1
ATTN RIBADEAU DUMAS MATRA DEFENSE 37 AV LOUIS BREGUET BP 1 78146 VELIZY VILLACOUBLAY CEDEX FRANCE	1
ATTN R ROGERS DEFENCE RESEARCH AGENCY BLDG 37 TUNNEL SITE CLAPHAM BEDS MK 41 6AE UNITED KINGDOM	1
ATTN S SMITH DEFENCE RESEARCH AGENCY Q134 BUILDING RAE FARNBOROUGH HAMPSHIRE QU14 6TD UNITED KINGDOM	1
ATTN J SOWA SAAB MISSILES AB 581 88 LINKOPING SWEDEN	1
ATTN D SPARROW HUNTING ENGINEERING LTD REDDINGS WOOD AMPTHILL BEDFORDSHIRE MK452HD UNITED KINGDOM	1
ATTN P STUDER DEFENCE TECHNOLOGY AND PROCUREMENT AGENCY SYSTEMS ANALYSIS AND INFORMATION SYSTEMS DIVISION PAPIERMUEHLESTRASSE 25 3003 BERNE SWITZERLAND	1
ATTN DR R G LACAU AEROSPATIALE MISSILE DEPT E/ECN CENTRE DES GATINES 91370 VERRIERE LE BUISSON FRANCE	1
ATTN J M CHARBONNIER VON KARMAN INSTITUTE 72 CHAUSSEE DE WATERLOO 1640 RHODE SAINT GENESE BELGIUM	1
ATTN P CHAMPIGNY DIRECTION DE L AERONAUTIQUE ONERA 29 AV DE LA DIVISION LECLERC 92320 CHATILLON SOUS BAGNEUX CEDEX FRANCE	1
ATTN DR P HENNIG DEUTSCHE AEROSPACE (DASA) VAS 414 ABWEHR AND SCHUTZ POSTFACH 801149 8000 MUENCHEN 80 GERMANY	1

DISTRIBUTION (Continued)

	Copies
ATTN H G KNOCHE	1
DR GREGORIOU	1
MESSERSCHMIDT BOLKOW BLOHM	
GMBH	
UNTERNEHMENSBEREICH APPARATAE	
MUNCHEN 80 POSTFACH 801149 BAYERN	
GERMANY	
INTERNAL	
B	1
B05 (STATON)	1
B44	1
B44 (HSIEH)	1
B44 (WARDLAW)	1
B51 (ARMISTEAD)	1
B60 (LIBRARY)	3
C	1
D	1
D4	1
G	1
G02	1
G04	5
G20	1
G205	1
G23	1
G23 (BIBEL)	1
G23 (CHADWICK)	1
G23 (COOK)	1
G23 (GRAFF)	1
G23 (HANGER)	1
G23 (HARDY)	1
G23 (HYMER)	5
G23 (MCINVILLE)	5
G23 (OHLMEYER)	1
G23 (RODRIGUEZ)	1
G23 (ROWLES)	1
G23 (WEISEL)	1
G30	1
G305	1
G32 (DAY)	1
G33 (MELTON)	1
G33 (RINALDI)	1
G40	1
G50	1
G50 (SOLOMON)	1
G60	1
G70	1
G72	1
K	1
K10	1
K20	1
K204	1
K22 (SATYA)	1
K44 (ICHNIOWSKI)	1
N	1
T	1